UNIVERSITY OF CALGARY

Measurement and Modeling of Asphaltene-Rich Phase Composition

by

Shinil George

A THESIS

SUBMITTED TO THE FACULTY OF GRADUATE STUDIES

IN PARTIAL FULFILMENT OF THE REQUIREMENTS FOR THE

DEGREE OF MASTER OF SCIENCE IN CHEMICAL ENGINEERING

DEPARTMENT OF CHEMICAL AND PETROLEUM ENGINEERING

CALGARY, ALBERTA

DECEMBER, 2009

UNIVERSITY OF CALGARY

FACULTY OF GRADUATE STUDIES

The undersigned certify that they have read, and recommend to the Faculty of Graduate Studies for acceptance, a thesis entitled " Measurement and Modeling of Asphaltene-Rich Phase Composition" submitted by Shinil George in partial fulfilment of the requirements of the degree of Master of Science in Chemical Engineering.

Supervisor, Dr. Harvey W. Yarranton
Department of Chemical and Petroleum Engineering

Dr. William Y. Svrcek
Department of Chemical and Petroleum Engineering

Dr. Marco A. Satyro
Department of Chemical and Petroleum Engineering

Dr. Ed Nowicki
Department of Electrical and Computer Engineering

Date

Abstract

Oil producers are beginning to consider solvent-based or solvent-assisted processes to recover heavy oil. To design these processes, it is necessary to predict the amount and composition of the phases that form when the heavy oil and solvent mix. In particular, the formation of asphaltene-rich phases can strongly affect the recovery process.

A previously developed regular solution model successfully predicted the amount of asphaltenes in dense phases formed in solutions of asphaltenes, toluene, and n-alkanes as well as in heavy oils diluted with n-alkanes. However, this model assumed that there is no solvent partitioning to the asphaltene-rich phase, which is thermodynamically incorrect. Furthermore, no compositional data for the asphaltene-rich phase was available with which to tune the model.

A new experimental approach was developed to calculate the composition of solvent in the asphaltene-rich phase. The experiments were based on the difference between the evaporation rate of the free or entrained solvent versus that of the solvent dissolved in the asphaltene-rich phase. The mass of a mixture of asphaltenes and solvent was measured over time and there was a clear and consistent change in slope when the entrained solvent evaporation ended. The amount of solvent in the asphaltene-rich was determined at this point.

A previously developed regular solution model was modified to include all components in the asphaltene-rich phase to take part in the phase equilibrium. The model was re-

tuned using n-heptane/toluene/Athabasca asphaltene data. The model predicted reasonably good results for fractional precipitation of asphaltenes having different average molar mass, except for the low molar mass asphaltenes. The predictions for different n-alkane solvents were less accurate particularly for heavy solvents n-octane and n-decane. The model did not handle the effect of asphaltene concentration well. The revised model also significantly over-predicted the solvent content of the asphaltene-rich phase.

Acknowledgements

I wish to express my sincere gratitude and thanks to my supervisor Dr. Harvey W. Yarranton for his invaluable guidance, encouragement and support throughout the program. It was a privilege for me to work with him. I also extend my heartfelt thanks to Dr. Marco A. Satyro for his help and guidance throughout this endeavour. He was very kind to allow me to use Virtual Materials group (VMG) software packages for the modeling work.

I express my sincere gratitude to the Asphaltene and Emulsion research group members for their support and cooperation. I am thankful to Asok Tharanivasan for the fruitful discussions that contributed to this thesis. I like to acknowledge the help of Elaine Baydak for her help during my experimental work. Further, I would like to thank NSERC and Department of Chemical and Petroleum Engineering for the funding support. Finally, I am indebted to my family, especially to my wife Golda for their love and unwavering support.

Dedication

To

My family

Table of Contents

List of Tables

List of Figures and Illustrations

List of Symbols, Abbreviations and Nomenclature

f	Fugacity
K	Equilibrium ratio
M	Molar mass
P	Pressure
R	Universal gas constant
T	absolute temperature (K)
V	Volume
v	Molar volume
x	Mole fraction
z	Mole fraction of the feed

Greek symbols

Δ	Difference
Γ	Gamma function
α	Shape factor in distribution function
δ	Solubility parameter
ε	Overall error
μ	Chemical Potential
ρ	Density
γ	Activity coefficient
ϕ	Volume fraction

Subscripts and Superscripts

aro	aromatics
curr	current iteration
i	Component
L1	Light liquid phase
L2	Heavy liquid phase

m	Mixture
prev	previous iteration
ref	reference
sat	saturates
vap	vaporization

Chapter One: Introduction

With conventional crude oil resources depleting rapidly, there has been a gradual shift in focus towards the exploration and processing of heavier crude oils and bitumen. These heavier crudes are commonly found in places such as Canada (Alberta and Saskatchewan) and Venezuela. In Alberta, the primary source of bitumen is oil sands deposits which are located in the north-eastern area of the province. Shallow deposits are mined and the bitumen is extracted using a hot water process primarily the Clark hot water process (Chastko, P. A., 2005). Deeper deposits are produced using a variety of methods including cold production, steam assisted gravity drainage, and cyclic steam stimulation.

Heavy oil is more difficult to produce and process when compared to the conventional oil because it has a higher density and viscosity as well as higher sulphur and metals content and residue fraction. Usually, heavy oil requires processing to remove metals and increase the hydrogen content before it can be sent into a conventional downstream refinery. The processing and transportation of bitumen also requires the reduction of viscosity by the addition of diluents or increasing the temperature. The diluents normally added are naphtha or condensate consisting generally of pentanes and higher carbon number compounds. The addition of such solvents can precipitate asphaltenes. Asphaltenes are the heaviest, most polar fraction of a heavy crude oil and are defined as a solubility class of materials that are insoluble in an n-alkane (usually n-pentane or n-heptane) but soluble in aromatic solvents such as toluene.

1.1 Asphaltene Precipitation

The heavy oils and bitumen found in Western Canada contain a high percentage of asphaltenes (Ignasiak, T., et al., 1979). Asphaltenes can precipitate from a crude oil due to a change in pressure, temperature, or composition. For example, for relatively light oils which contain some asphaltenes, asphaltene precipitation can occur in the wellbore due to a reduction in pressure. This type of precipitation primarily occurs in highly under-saturated reservoirs. With heavy oils, asphaltenes can precipitate when the oil is diluted with solvents to reduce the viscosity. Blending of incompatible crude oils during transport or in a refinery can also lead to asphaltene precipitation.

In some processes asphaltene precipitation is desirable. One such example is the Albian process, where a paraffinic solvent is added to the froth to reduce the bitumen density and viscosity and to promote flocculation of the emulsified water and suspended solids. Some asphaltenes are precipitated in the process to achieve a product suitable for processing in a conventional refinery (Romanova et al., 2004).

However, asphaltene precipitation has many undesirable effects on oil production during miscible flooding, heavy oil recovery, or even primary depletion (Qin, X., et al., 2000). Asphaltene can also precipitate during Enhanced Oil Recovery (EOR) methods such as gas and CO2 injection. Many operating problems are encountered during the production, transportation and refining of heavy oil due to the precipitation of asphaltene. Oil production is often reduced when asphaltenes precipitate because they plug the pores of

the reservoir. Asphaltene deposition likely involves several steps including precipitation, flocculation, adsorption, and adhesion (Alboudwarej et al., 2004). The deposition of asphaltenes can hinder flow in pipelines and damage pumps which results in reduced production and increased downtime. The presence of asphaltenes increases the pressure drop through the pipeline, which leads to increase in the pumping costs. The precipitated asphaltenes can also cause problems in the downstream refinery equipment. They can reduce the activity of catalysts used in the downstream processes such as Fluidized Catalytic Cracking (FCC) and Hydrocracking, by adsorbing on the surface of the catalyst. Asphaltene deposition during production and processing of oil ranks as one of the costliest technical problems the petroleum industry faces (Leontaritis and Mansoori, 1987).

The problems related to asphaltenes are generally not known until the exploration phase or in some cases, development phase of the oil discovery. For this reason, oil producers do not encounter these problems until a large portion of the ultimate capital expenditure is spent on developing the fields. Hence, it is important for the producer to be able to predict the potential asphaltene related problems before the start of the project. In fact, the prediction of asphaltene precipitation could be a crucial factor in the decision to develop the field (Leontaritis and Mansoori, 1987).

1.2 Modeling Asphaltene Precipitation

The regular solution approach has been shown to provide good predictions of asphaltene precipitation from heavy oils (Akbarzadeh et al., 2005) and was chosen as the modeling

approach for this thesis. Hirschberg et al. (1984) was the first to apply this approach to asphaltenes. He treated the asphaltenes as a polymer and used the Flory-Huggins polymer solution theory to model the asphaltene solubility in crude oil. Yarranton and Masliyah (1996) modeled asphaltene precipitation in solvents by treating asphaltenes as a mixture of components of different density and molar mass. Alboudwarej et al. (2003) and Akbarzadeh et al. (2005) used regular solution theory to model precipitation from asphaltene/toluene/n-alkane system and diluted bitumen. While these models provided good predictions of asphaltene yields, they were simplified with the assumption that only asphaltenes and resins partition to asphaltene-rich phase. This assumption allowed for easier convergence of the flash calculations; however, it is thermodynamically incorrect as lighter components and solvents must be free to partition to the asphaltene-rich phase.

1.3 Objectives and Thesis Structure

The aim of the thesis is to modify the previously developed regular solution model to include all components to partition to the asphaltene-rich phase (heavy liquid phase). Data on the amount and composition of the asphaltene-rich phase are required to test the model predictions. Yield data was obtained from Akbarzadeh et al., 2005, Alboudwarej et al., 2002 Yarranton et al., 1996 and Mannistu et al., 1997. However, data on the composition of the asphaltene-rich phase are scarce. Therefore, the specific objectives of this thesis are to:

1. measure the solvent content in the asphaltene-rich phase.
2. modify the regular solution model to allow all components to partition to both phases.

This thesis consists of the following chapters.

Chapter 2 reviews the relevant literature on crude oil characterization, asphaltene chemistry, asphaltene self association, asphaltene precipitation and asphaltene-rich phase composition. This chapter also discusses the regular solution approach to modeling asphaltene precipitation.

Chapter 3 details the experimental work employed in this study. The approach developed to determine the composition of solvent in the asphaltene-rich phase is discussed.

Chapter 4 describes the modeling work performed using the regular solution theory. The chapter explains how the existing model is modified to allow all components to partition to both phases. The fluid characterization and the flash calculations are also explained.

Chapter 5 presents the results of the experiments for determining the solvent content in the asphaltene-rich phase. The experiments were performed for asphaltene/toluene/n-alkane and diluted bitumen systems.

Chapter 6 discusses the modeling results for asphaltene/ toluene/n-alkane system. The results of the old model are included for comparison. The effect of solvents, asphaltene molar mass and asphaltene source are discussed. The model predictions for the solvent content of the asphaltene-rich phase are compared with the experimental data.

Chapter 7 summarizes the conclusions of this study and provides recommendations for future work. The error analysis of the experimental and modeling results is included in an appendix.

Chapter Two: Literature Review

In this chapter, an introduction to crude oil is provided. The major oil characterization methods are reviewed. The chemistry of crude oil fractions (saturates, aromatics, resins, and asphaltenes) are discussed with a focus on asphaltene self-association and precipitation. Regular solution based models for asphaltene phase behaviour are reviewed. Finally, recent research on the modeling of asphaltene-rich phase compositions is presented.

2.1 Conventional Crude Oils and Bitumen

Crude oil is a complex mixture of thousands of hydrocarbons with different carbon number, molecular structures and sizes. Petroleum reservoir fluids may contain hydrocarbons as heavy as C_{200} (Pedersen et al., 2007). They may also contain many inorganic compounds of which nitrogen, sulphur, and carbon dioxide are the most significant from a refining perspective. Other inorganic constituents include water, salts, metals, silicates, and clays.

Crude oils are often described in terms of API (American Petroleum Institute) gravity. API density is the measure of density of the crude oil relative to density of water. The higher the API gravity, the lighter is the crude oil.

$$^{\circ}API = \frac{141.5}{\mathrm{SG}} - 131.5 \qquad \textbf{(2-1)}$$

where SG is the specific gravity of the oil. Heavy oils and bitumen are defined based on both their density and their viscosity, as shown in **Table 2-1**.

Table 2-1: UNITAR definitions of oils and bitumens (Gray, 1994)

Type	Viscosity (mPa.s)	Density (kg/m^3)
Conventional Oil	$< 10^2$	< 934
Heavy Oil	10^2-10^5	934-1000
Bitumen	$> 10^5$	> 1000

2.2 Crude Oil Characterization

Crude oil is a collection of thousands of components and it is impossible to carry out a complete component analysis. Instead, lumping methods are used to describe the characteristics of the fluid. The properties of a collection of components are determined, instead of a single component.

2.2.1 Distillation Methods

Conventional crude oils are typically characterized based on distillation curve and compositional analysis of the lighter end hydrocarbons. The oil is usually divided into cut points, which are subdivisions of distillation curve, usually based on boiling point ranges. The density and molecular weight of each distillation cut are measured using analytical methods. Since there are limited number of carbon atoms in a distillation cut, its molecular weight can be measured with a higher accuracy than the average molecular

weight of the oil sample as a whole (Pedersen, et al., 2007). These analytical results become part of the "Petroleum Assay".

The pressure is reduced during distillation for certain characterization methods to avoid thermal decomposition or cracking. The endpoints of the boiling range corresponding to a particular cut are known as the cut points and each of the cuts is termed a pseudo-component or hypothetical component. The pseudo-components' properties are estimated based on established methods and correlations.

The approach of "cutting" a distillation curve based on boiling points works well for conventional crude oils. This is because the non-distillable fractions are small, typically less than 5 wt % of the oil. But the approach does not work well for heavy oils and bitumens where approximately 60% of the oil is non-distillable (Nji, et al., 2008). This entails the use of some alternative techniques to characterize heavy oils and bitumen.

2.2.2 SARA fractionation

One approach is to separate the crude oil into four components based on solubility and adsorption classes. The method is called SARA fractionation and the four components are saturates, aromatics, resins, and asphaltenes. The SARA fractions are explained in more detail below.

2.2.2.1 Saturates

Saturates consist of normal alkanes (n-paraffins), branched alkanes (iso-paraffins) and cycloparaffins. Paraffins are hydrocarbon groups of the type C, CH, CH2 or CH3. The carbons atoms are connected by single bonds with no cyclic chains. Cycloparaffins are similar to paraffins in the sense that that are comprised of the same type of hydrocarbon groups, but differ from paraffins by containing at least one cyclic structure. They are also called naphthenes. The single-ring naphthenes present in petroleum are primarily alkyl-substituted cyclo-pentanes and cyclo-hexanes (Speight, 1999). Saturates are the least polar among the SARA fractions. The molar mass of saturates is in the range of 361 g/mol to 524 g/mol and their density is found to vary in the range of 853 to 900 kg/m³. (Akbarzadeh et al., 2005)

2.2.2.2 Aromatics

Aromatics contain one or more cyclic structures similar to naphthenes, but the carbon atoms in an aromatics compound is connected by aromatic double bonds; that is, they are like benzene rings. Polycyclic aromatic compounds with two or more ring structures are also found in the aromatic, resin, and asphaltene fractions. The molar mass of aromatics is in the range of 450-550 g/mol. The densities are reported to vary from 960 to 1003 kg/m³ (Akbarzadeh et al., 2005).

2.2.2.3 Resins

Resins are polycyclic aromatics with higher molar mass, density, aromaticity, and heteroatom content than the aromatics. They are thought to be molecular precursors of

the asphaltenes but, unlike asphaltenes, are soluble in pentane (Speight, 1999). Resins are chemically similar to asphaltenes and are assumed to be soluble in the crude oil (Hammami and Ratulowski, 2007). Resins can be converted to asphaltenes by oxidation with atmospheric oxygen (Speight, 1999).

The molar mass of resins varies from 859 to 1240 g/mol. The molar mass is much higher than aromatics, but substantially lower than asphaltenes. However, the molar mass comparisons may be misleading because the asphaltenes and possibly the resins self-associate. The densities reported are in the range of 1007 to 1066 kg/m^3 (Akbarzadeh et al., 2005).

2.2.2.4 Asphaltenes

Asphaltenes are defined as the components of crude oil that are soluble in aromatic solvents such as toluene, but insoluble in n-alkane solvents like n-heptane. Some asphaltene species are even insoluble in crude oil. The bitumen components excluding asphaltenes (the saturates, aromatics and resins) are called maltenes.

Asphaltenes are mixtures of many thousands of chemical species and their structure is not readily identified. They are generally composed of polynuclear aromatic rings, aliphatic side chains and heteroatom such as nitrogen, sulphur and oxygen. The number of rings varies from 6 to 15 (Simanzhenkov and Idem, 2003). They have the highest molar mass, aromaticity and heteroatom content of all the crude oil components (Wiehe et al., 1996). They are also the most polar fraction among all the crude oil components.

Asphaltenes are responsible for the high density and viscosity of heavy crudes and bitumen. The average monomer molar mass of asphaltenes is in the range of 750 to 1800 g/mol (Yarranton et al., 2000, Badre et al., 2006) with recent data suggesting a value of approximately 1000 g/mol (Pinkston et al., 2009). The apparent molar mass of self-associated asphaltenes is in the order of 5000 to 10000 g/mol and perhaps higher (Yarranton et al., 2000). The densities reported are in the range of 1132 to 1193 kg/m^3 (Akbarzadeh et al., 2005).

There are two different structures proposed for asphaltenes. The continent or pericondensed structure is formed by molecules with large "continent" of aromatic rings extended by short aliphatic chains. The archipelago model suggests asphaltenes as a collection of small aromatic islands interconnected by aliphatic chains.

The hypothetical structure of a representative archipelago-like asphaltene molecule is depicted in Figure 2.1 (Strausz et al., 1992).

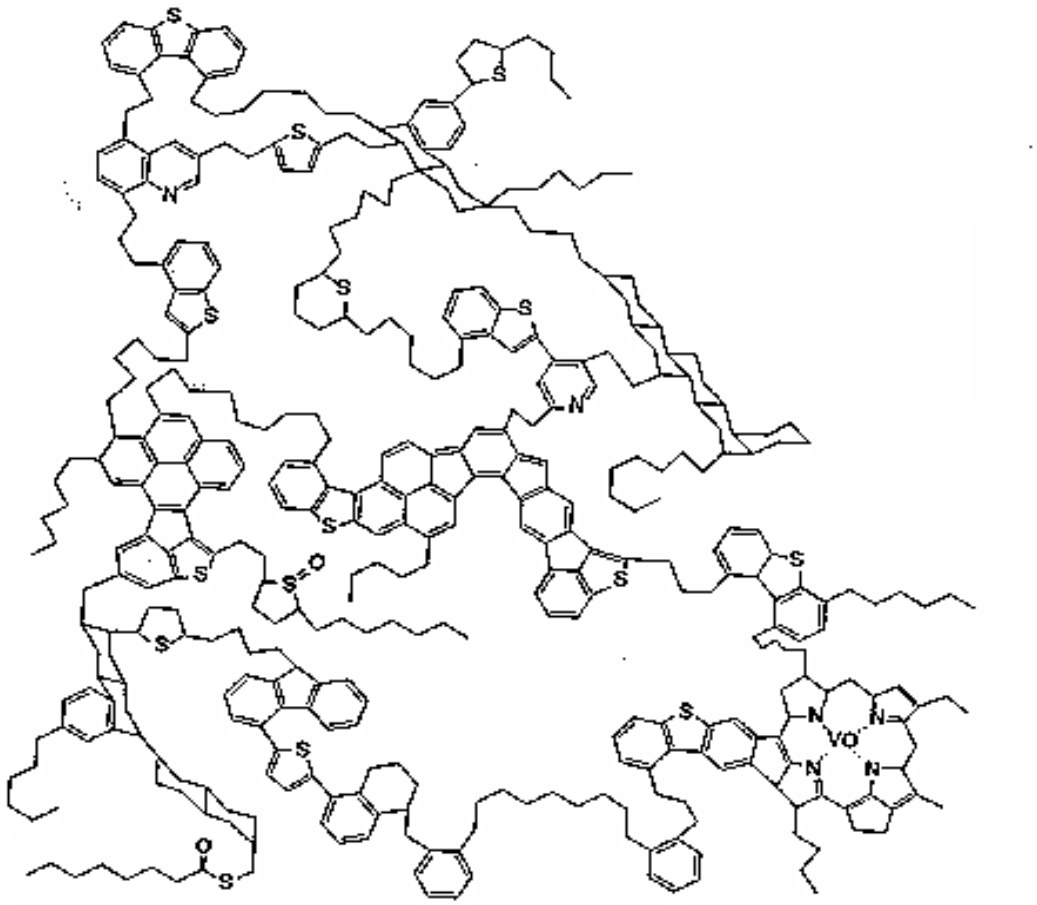

Figure 2.1: Hypothetical model of a simplified Athabasca asphaltene molecule (Strausz et al., 1992).

2.3 Asphaltene Association

Asphaltenes have a strong tendency to self-associate and likely exist as unassociated molecules only in very dilute solutions of "good" solvents (Buckley et al., 2007). Vapour pressure osmometery data indicates that asphaltenes self-associate into aggregates

consisting of approximately 2 to 6 molecules per aggregate in aromatic solvents (Yarranton et al., 2000).

The aggregates have been considered as colloidal particles (Pfeiffer et al., 1940) or macromolecules (Hirschberg et al., 1984). With the colloidal view, the asphaltenes are considered to be a colloidal suspension in the crude oil. The associated asphaltenes are considered to form a stack which is surrounded and dispersed in the oil by resins.

With the macromolecular view, the asphaltene is considered to be completely dissolved in the crude oil. The associated asphaltenes are independent molecules similar to the resins and other crude oil constituents. Recent literature favours the macromolecular view based on molar mass and calorimetric experiments (Andersen, 1999; Agrawala and Yarranton, 2001 and Peramanu et al., 2001).

Agrawala and Yarranton (2001) proposed that molecules of asphaltenes aggregate in a manner analogous to linear “polymerization”. In this process, the interactions between free asphaltene molecules have been described in terms of two distinct classes. Some molecules may contain several active sites and therefore propagate aggregation (propagators). Other molecules may contain only one site and therefore terminate further growth (terminators). Asphaltenes consist mainly of propagators, while resins consist mainly of terminators. This approach was used to explain the observed asphaltene molar mass distributions and the inhibiting effect of resin or asphaltene molar mass.

The above model was improved to include both asphaltenes and resins as a mixture of self-associating species (Yarranton et al., 2007). Their results suggested that resins also participate in asphaltene self-association and the fit of the solubility curves improved with the new model. It was concluded that the asphaltenes and resins are best characterized as a single continuum of aggregated species.

2.4 Asphaltene Precipitation

In a reservoir, asphaltenes precipitate at a certain range of temperature and pressure. As shown in **Figure 2.2**, at isothermal conditions, when pressure drops and reaches point A, asphaltenes begin to precipitate. The amount of precipitation may change with pressure until it reaches point B, where asphaltenes disappear (Qin, et al., 2000).

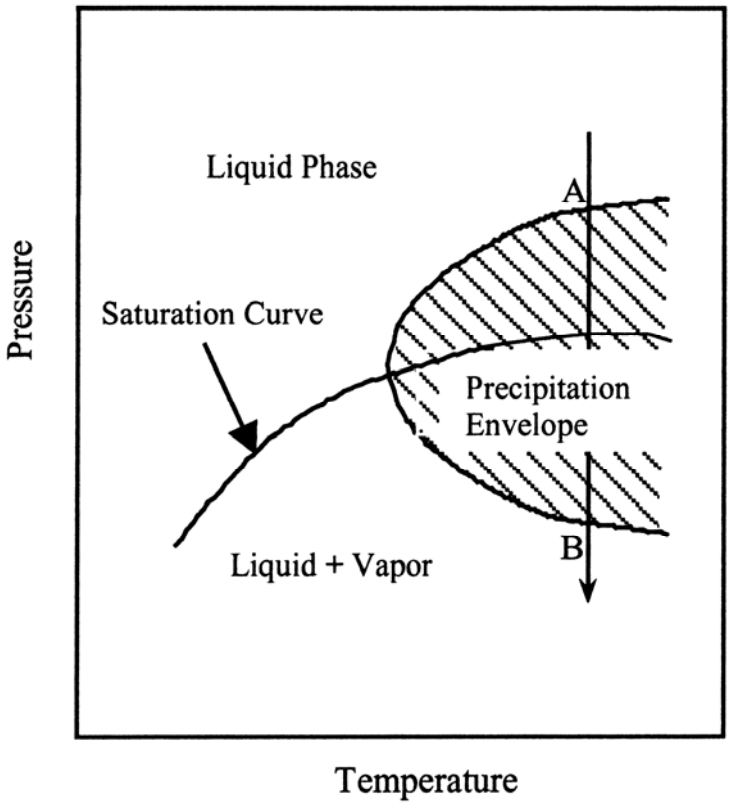

Figure 2.2: Asphaltene precipitation envelope (Qin, X., et al., 2000).

When bitumen is diluted with an n-alkane, or other non-aromatic solvents, asphaltene precipitation occurs. Mitchell et al. (1973) showed that solvent power, which is the ability of the solvent to dissolve asphaltenes, increases in the order: 2-methyl paraffin < n-paraffin < terminal olefin. This means 2-methyl paraffin solvents precipitate more asphaltene than n-paraffin and terminal olefin solvents. They proved that cycloalkanes and their methyl derivatives have solvent powers similar to those of aromatics. The aromatic character of the asphaltenes and their content of heteroatoms are the main influence on their solubility in different solvents and their tendency to flocculate (Browarzik and Browarzik, 2005). Overall, the parameters that govern precipitation

appear to be the composition of the crude oil, pressure, temperature and properties of asphaltenes (Hirschberg et al., 1984).

There is some debate in the literature on the reversibility of asphaltene precipitation. Studies from titration experiments where asphaltenes are precipitated with precipitant and then re-dissolved through solvent addition demonstrated that full reversibility did not occur (Andersen, 1992). However, Peramanu (2001) concluded that precipitation could be completely reversed as long as there is sufficient turbulence to break up the asphaltene particles. Beck et al. (2005) showed that there is a hysteresis in asphaltene re-dissolution that could be overcome with the removal of a poor solvent. Zou and Shaw (2004) showed that bulk phase behaviour of hydrocarbon mixtures containing asphaltenes is reversible, by conducting phase behaviour experiments on diluted Athabasca bitumen.

Precipitated asphaltenes manifest as approximately micron sized particles (Rastegari et al., 2004) and form a black powder upon drying. However, asphaltenes likely undergo a liquid-liquid phase separation from solution (Sirota, 2005). Sirota explained that the solid-like character of the asphaltene-rich phase is only due to the fact that the material in the heavier phase is below its glass-transition temperature. Therefore the current evidence suggests that asphaltenes are indeed liquids, which may be in a glassy state depending on the system temperature. Hirschberg et al. (1984) proposed a qualitatively accurate liquid-liquid equilibrium model for the phase behaviour of asphaltene precipitation. This has led to the LLE assumption in many of the newer models.

2.5 Modeling of Asphaltene Precipitation

There are two types of modeling approaches commonly used for describing asphaltene phase behaviour, colloidal and thermodynamic models. The colloidal model was the first proposed but thermodynamic models have proved more successful at predicting phase behaviour.

2.5.1 Colloidal Model

Nellensteyn (1924) inferred a colloidal structure for bitumen based on observations such as the Tyndall effect and Brownian motion of particles. He observed that an asphalt-like dispersion could be prepared from asphalt base oil using a dispersion of finely divided elemental carbon. Pfeiffer and Saal (1940) created a model to explain the rheological observations consistent with the colloidal nature of bitumen by extending Nellensteyn's work. They proposed insufficient resin coating as the cause of asphaltene flocculation.

Leontaritis et al. (1987) proposed a model based on statistical thermodynamics and colloidal science techniques to predict asphaltene precipitation in crude oil. The model assumed that asphaltenes exist in the oil as solid particles in colloidal suspension, stabilized by resins adsorbed on their surface. They also assumed that short range intermolecular repulsive forces between resin molecules adsorbed on different asphaltene particles keeps them from flocculating. Therefore, the phase behaviour depends on the chemical potential of the resins:

$$\mu_{resin}^{asphaltene\,.\,phase} = \mu_{resin}^{oil\,.\,phase} \qquad \textbf{(2-2)}$$

where $\mu_{resin}^{asphaltene.phase}$ and $\mu_{resin}^{oil.phase}$ are the chemical potential of resin in the asphaltene phase and the oil phase respectively. The chemical potential of resin can be calculated from a regular solution model coupled with the Flory-Huggins entropy contribution from statistical thermodynamics theory as follows:

$$\frac{\mu_i - \mu_i^{ref}}{RT} = \ln\left(\frac{x_i v_i}{v_m}\right) + 1 - \frac{v_i}{v_m} + \frac{v_i}{RT}\left(\delta_m - \delta_i\right)^2 \qquad \textbf{(2-3)}$$

where μ_i and μ_i^{ref} are the chemical potential of component *i* and reference chemical potential; v_i and v_m are the molar volumes of the component *i* and mixture respectively and δ_m and δ_i are the solubility parameters of the mixture and component *i*, respectively. *R* is ideal gas constant and *T*, the absolute temperature.

It was assumed that chemical potential of resins in the solid and liquid phases determined the split between the two phases. The concentration of resin in the liquid which is just enough to stabilize the colloidal asphaltene particles is called critical resin concentration (Cr^{crit}) and the chemical potential at this point is called the critical resin chemical potential (μ_r^{crit}) . Given the critical resin concentration of a particular oil mixture, resin and oil properties, the critical chemical potential can be found using the above equation. If the actual resin chemical potential (μ_r) is less than to the μ_r^{crit}, asphaltene flocculation is possible. With this method, the minimum amount of solvent needed to start flocculation can be calculated.

The colloidal model is not consistent with liquid-liquid equilibrium and predicts that asphaltene precipitation is irreversible. Colloidal model can fit the onset point of asphaltene precipitation upon addition of a poor solvent but cannot predict the yield (Janardhan and Mansoori, 1993). Cimino et al (1995) observed that the physical basis of colloidal model is not correct, as asphaltenes could be dissolved in solvents without the presence of resins.

2.5.2 Thermodynamic Models

The thermodynamic approach assumes that self-associated asphaltenes behave as macromolecules in solution. These macromolecules can undergo a conventional phase change to form a solid or dense liquid phase. The thermodynamic approach has been successful in modeling asphaltene precipitation over a range of temperatures and pressures. The thermodynamic approach can also model both the onset point of asphaltene precipitation and asphaltene yield. Of the many approaches to modeling asphaltene precipitation, the regular solution and equation-of-state approaches are the most common. This thesis focuses on regular solution models and, therefore, equation-of-state approaches are not reviewed.

2.5.3 Modified Regular Solution Theory

Hirschberg et al. (1984) treated the asphaltene precipitation analogous to liquid-liquid equilibrium of a polymer solution. They combined Flory-Huggins theory with the solubility concept to express the volume fraction of the asphaltene dissolved in the oil (ϕ_a).

$$\phi_a = \exp\left\{\frac{v_a}{v_L}\left[1-\frac{v_L}{v_a}-\frac{v_L}{RT}\left(\delta_a-\delta_L\right)^2\right]\right\} \quad \textbf{(2-4)}$$

where v_a and v_l denote asphaltene molar volume and oil molar volume respectively. δ_L and δ_A are the solubility parameter of the mixture and the asphaltene respectively.

Vapour-Liquid equilibrium calculations were performed using the Soave-Redlich−Kwong (SRK) equation of state. The calculations were performed mainly to calculate the composition of the liquid phase and it was assumed that there was no asphaltene precipitation during the vapour/liquid equilibrium (VLE) calculations. Once the liquid phase compositions were known, the asphaltene precipitation was predicted using modified Flory-Huggins theory, assuming that the precipitation does not change the vapour/liquid equilibrium. The heavy liquid phase was assumed to be pure asphaltene.

Cimino et al. (1995) modified Hirschberg model by assuming that solvent also forms part of the heavy liquid phase, not just asphaltenes. They neglected the asphaltene fraction in the light liquid phase and derived the equation for calculating the activity coefficient of asphaltenes:

$$\ln\left(1-\phi_a^*\right)+\left(1-\frac{v_s}{v_a}\right)\phi_a^*+\frac{v_s}{RT}\left(\delta_a-\delta_s\right)^2\phi_a^{*2}=0 \quad \textbf{(2-5)}$$

where v_s is molar volumes of asphaltenes and oil (considered as solvent for asphaltenes) respectively. ϕ_a^* is asphaltene volumetric fraction in the nucleating phase at the onset of

flocculation. The above equation can be used for finding the onset point of asphaltene precipitation, but it cannot predict the asphaltene yield. In fact, all the asphaltene is precipitated at the onset point because the solvent phase is assumed to be pure.

Browarzik et al. (1999) modeled the asphaltene system using solubility parameters. They argued that, molar mass is not suitable for characterizing heavy oil or asphaltene since the molar mass measurement is not very accurate. Furthermore, the molar mass measurements are affected by the experimental conditions like choice of solvent and temperature. Therefore, the solubility parameter of the Scatchard–Hildebrand theory was selected as a more convenient identification variable for the oil species than the molar mass. The solubility parameter reflects the intermolecular interactions originating from the aromaticity and the heteroatoms in some way. A further reason for the oil characterization using the solubility parameter is the possibility to correlate it with experimentally available data.

They used a correlation for calculating the solubility parameter, which is a function of the number of carbon atoms and of the hydrogen deficit. The calculation of the solubility parameter of oil needs only experimental values of the molar mass average and the content of carbon, hydrogen and heteroatoms. They results were reasonable when compared with the measured flocculation data.

Alboudwarej et al. (2003) assumed liquid-liquid equilibrium between the heavy liquid phase and the light liquid phase. The equilibrium ratio, K_i^{hl}, for any component is calculated by the following equation.

$$K_i^{hl} = \frac{x_i^h}{x_i^l} = exp\left\{ \begin{array}{l} \frac{v_i^h}{v_m^h} - \frac{v_i^l}{v_m^l} + ln\left(\frac{v_i^l}{v_m^l}\right) - ln\left(\frac{v_i^h}{v_m^h}\right) + \\ \frac{v_i^l}{RT}\left(\delta_i^l - \delta_m^l\right)^2 - \frac{v_i^h}{RT}\left(\delta_i^h - \delta_m^h\right)^2 \end{array} \right\} \quad \textbf{(2-6)}$$

where x_i^h and x_i^l are the heavy and light liquid phase mole fractions, R is the universal gas constant, T is temperature, v_i and δ_i are the molar volume and solubility parameter of component i in either the light liquid phase (l) or the heavy liquid phase (h), and v_m and δ_m are the molar volume and solubility parameter of either the light liquid phase or the heavy liquid phase, respectively. The heavy liquid was assumed to comprise of resins and asphaltenes whereas the light liquid phase includes all the components.

It was further assumed that the heavy liquid phase is an ideal mixture. Therefore, the activity coefficients in the dense phase are unity. The above equation for equilibrium ratio can be simplified as

$$K_i = \gamma_i^{\,l} = \exp\left(\ln\frac{v_i^{\,l}}{v_m^{\,1}} + 1 - \frac{v_i^{\,l}}{v_m^{\,l}} + \frac{v_i^{\,l}}{RT}\left(\delta^l{}_i - \delta^l{}_m\right)^2 \right) \quad \textbf{(2-7)}$$

Bitumen was divided into four fractions corresponding to SARA fractions (saturates, aromatics, resins, and asphaltenes). The inputs to the model are the mole fraction, molar volume, and solubility parameter for each pseudo-component. Saturates, aromatics, and

resins were treated as individual pseudo-components. The asphaltenes were further divided into fractions of different molar mass. A molar mass distribution rather than 'lumping' as a single pseudo-component was used, which enabled matching the yield curve by changing the parameters of the molar mass distribution.

The gamma distribution function was used to describe the molar mass distribution:

$$f(M) = \frac{1}{\Gamma(\alpha)}\left[\frac{\alpha}{\left(\overline{M} - M_m\right)}\right]^{\alpha} \times \left(M - M_m\right)^{\alpha-1} \exp\left[\frac{\alpha\left(M - M_m\right)}{\left(\overline{M} - M_m\right)}\right] \qquad \textbf{(2-8)}$$

where M_m, and $\overline{M}$ are the monomer molar mass and average molar mass of asphaltenes, and α is a parameter which determines the shape of the distribution. $\Gamma(\alpha)$ is the Gamma function.

The molar volumes of the saturates and aromatics were determined from the measured molar masses and densities. The densities (and therefore molar volumes) of the asphaltenes and resins were correlated to molar mass (Alboudwarej et al., 2003):

$$\rho = 670\ M^{0.0639} \qquad \textbf{(2-9)}$$

where ρ is the asphaltene density in kg/m³ and M is the molar mass in g/mol.

The solubility parameter is defined as follows:

$$\delta = \left(\frac{\Delta H^{vap} - RT}{v}\right)^{1/2} \qquad \textbf{(2-10)}$$

where ΔH^{vap} is the heat of vaporization. The solubility parameters of saturates and aromatics were determined by fitting the solubility model to asphaltene-saturate-toluene and asphaltene-*n*-heptane-aromatics solubility data, respectively.

The solubility parameter of asphaltenes was determined using the semi-empirical correlation recommended by Yarranton and Masliyah (1996).

$$\delta = (A\,\rho)^{1/2} \qquad \textbf{(2-11)}$$

where δ is the solubility parameter in $MPa^{0.5}$ and A is the monomer heat of vaporization in kJ/g. The constant A was determined by fitting the model to one set of asphaltene-*n*-heptane-toluene precipitation data.

Akbarzadeh et al. (2005) modified the regular solution model by Alboudwarej et al. (2003) by developing several empirical correlations for calculating the model inputs thereby generalizing the existing model. They correlated the densities of saturates and aromatics to temperature by fitting the density data.

$$\overline{\rho}_{sat} = -0.6379\,T + 1069.54 \qquad \textbf{(2-12)}$$

$$\overline{\rho}_{aro} = -0.5943\,T + 1164.73 \qquad \textbf{(2-13)}$$

where $\overline{\rho}_{sat}$ and $\overline{\rho}_{aro}$ are the average densities of saturates and aromatics in kg/m^3, respectively and T is temperature in Kelvin. The above correlations were validated on a number of heavy oils and bitumens.

The following correlations were developed to estimate the solubility parameters of saturates and aromatics at different temperatures:

$$\delta_{sat} = 22.381 - 0.0222\ T \quad \textbf{(2-14)}$$

$$\delta_{aro} = 26.333 - 0.0204\ T \quad \textbf{(2-15)}$$

where δ_{sat} and δ_{aro} are the solubility parameters of saturates and aromatics in $MPa^{0.5}$ and T is temperature in Kelvin.

The following correlation was used for the solubility parameter of n-alkanes at different temperatures:

$$\delta_{s,T} = \delta_{s,25} - 0.0232\ (T - 298.15) \quad \textbf{(2-16)}$$

where $\delta_{s,T}$ is solvent solubility parameter at temperature T, $\delta_{s,25}$ is solvent solubility parameter at 25°C estimated from Equation 2-10, and T is temperature in Kelvin.

The A parameter of Equation 2-11 was modified to be temperature dependent. The following correlation for A was determined by fitting the model to precipitation data for mixtures of asphaltene-heptane-toluene at temperatures of 23 and 50°C:

$$A(T) = -6.667 \times 10^{-4} T + 0.5614 \quad \textbf{(2-17)}$$

The modified regular solution model was able to predict the onset point of precipitation and asphaltene yields for a wide range of heavy oils and bitumen. The model was able to predict the temperature and pressure effects as well.

2.6 Asphaltene-Rich Phase Composition

At equilibrium, the asphaltene-rich phase must contain all the components present in the crude oil. However, such compositional data is rare. Hence, phase behaviour models for these systems are at least partially speculative because the predictions cannot be validated with experimental data for the composition of the asphaltene-rich phase. It can be concluded that asphaltene-rich phase behaviour is not clearly understood (Zou and Shaw, 2004).

There have been efforts to model the composition of asphaltene-rich phase in the literature. Szewczyk and Behar (1999) described asphaltene precipitation as a thermodynamic transition of asphaltenes from a first liquid phase, the crude, to a second liquid phase, the asphaltenic deposit which possibly includes all the components initially in the fluid before the phase separation. In his paper, crude oil was divided into a series of components and pseudo-components (F10-, F11-F20, Sat F20+, Aro F20+, resins and asphaltenes) for the purpose of modeling. The physical properties of the components were used directly and those of the pseudo-components were estimated using correlations based on the experimental values of density, molecular weight, and aromaticity. The amount and composition of the gas, liquid and asphaltenic phases were calculated by a single phase flash calculation using a volume translated Peng-Robinson EoS model and group contribution mixing rules. Since the thermodynamic model was not predictive, the proposed method consisted of fitting some physical characteristics (such as the critical properties of some pseudo-components and asphaltene molar mass) to data (crude oil relative volume, density of pseudo-components and solubility of asphaltene). The model

considered only the initial crude oil composition, avoiding the errors resulting from the assumption that asphaltene-rich phase is pure asphaltene. The composition of the asphaltene-rich phase was calculated by the flash procedure.

The results of the model are given in **Figure 2.3**. As expected, the majority of the asphaltenic deposit is composed of asphaltenes (approximately 85 wt%). The light fraction F10- is relatively significant and its weight percent is in the range of 5 wt%. The resin percentages are found to very low. They compared their results with an analysis of Venezuelan deposits and reported that there was good agreement although the data were not presented.

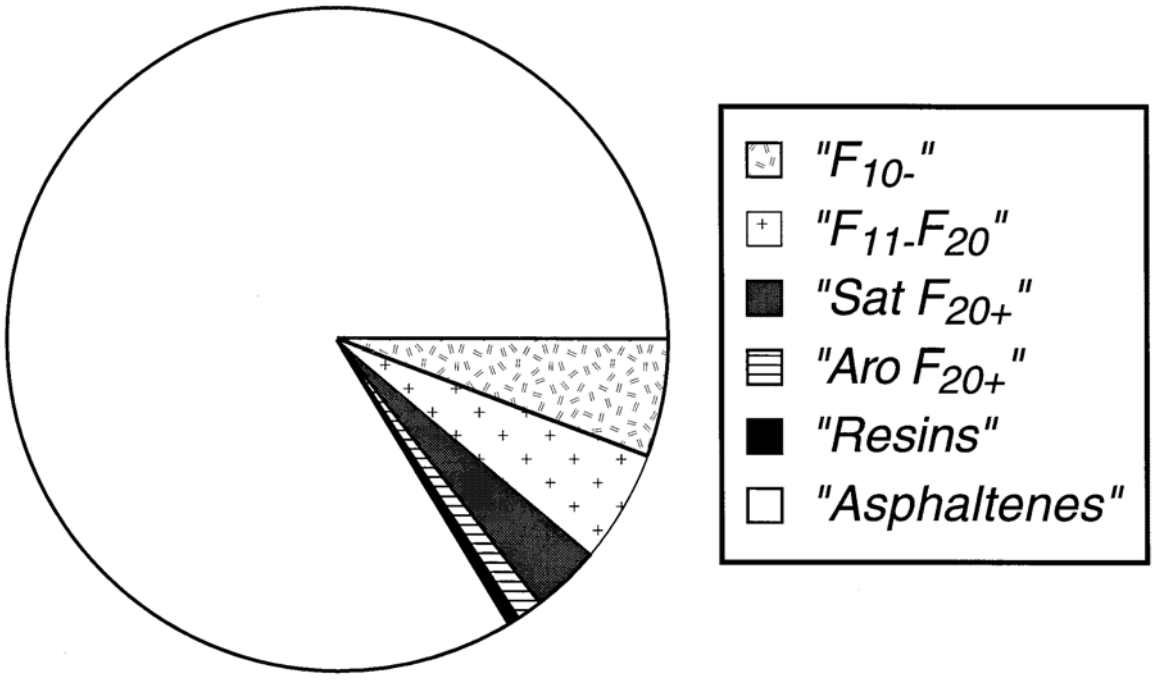

Figure 2.3: Calculated weight percent of the asphaltenic deposit at the saturation pressure and 303 K as predicted by the model by Szewczyk and Behar (1999).

Wu et al. (1998) proposed a model based on SAFT association model and colloidal theory. They assumed that asphaltenes and resins can be represented by pseudo-pure components, and that all other components in the crude oil can be represented by a continuous medium that effects interactions among asphaltene and resin molecules. The effect of the medium on asphaltene-asphaltene: resin-asphaltene, resin-resin pair interactions is taken into account through its density and dispersion-force properties. The expressions for the chemical potential of asphaltene and for the osmotic pressure of an asphaltene-containing solution was found using the SAFT model which is used in the framework of McMillan-Mayer theory which assumes hard-sphere repulsive, association and dispersion-force interactions. By assuming that asphaltene precipitation is a liquid-liquid equilibrium process, the model could describe precipitation of asphaltene from crude oil.

The framework could theoretically explain a variety of experimental observations, but quantitative predictions require molecular parameters that must be estimated from little experimental data. **Figure 2.4** shows the model predictions of the composition of asphaltene rich phases and solvent rich phases. However, the results are not compared with any experimental data. The predicted phase compositions are shown in **Table 2-2**.

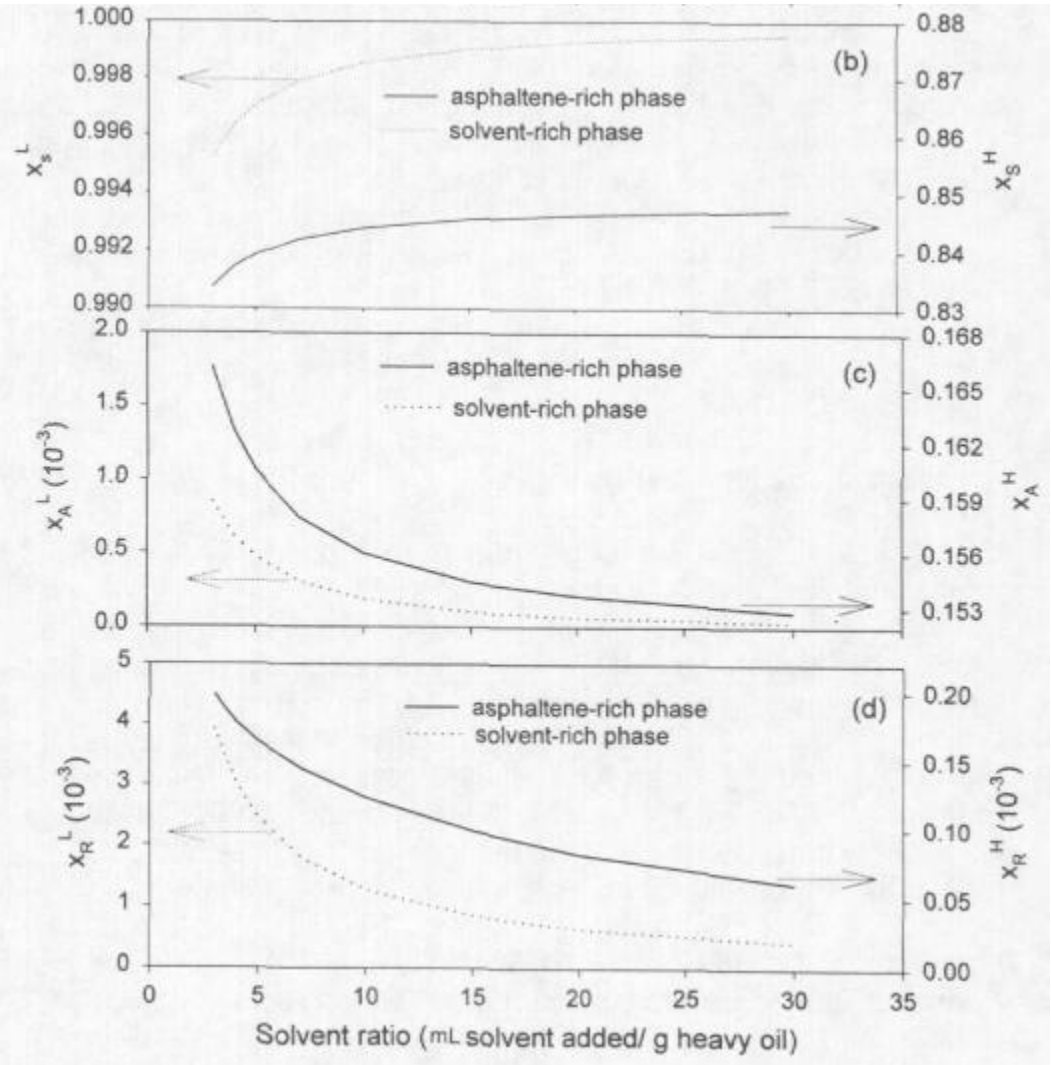

Figure 2.4: Composition (mole fractions) of asphaltene rich phase and solvent rich phase for Suffield oil at ambient temperature and pressure (Wu et al., 1998).

Table 2-2: Composition of asphaltene rich phase from Wu et al. (1998)

Composition (mole fraction) of solvent in asphaltene-rich phase	Composition (mole fraction) of asphaltene in asphaltene-rich phase
0.83 – 0.85	0.17 – 0.15

2.7 Summary

Asphaltenes can precipitate when there is a pressure depletion or when diluents are added to enhance its transportability. Regular solution models have been widely used to study asphaltene phase behaviour. The model developed by Alboudwarej et al (2003) and Akbarzadeh et al (2005) can successfully predict the precipitation of asphaltene after some initial tuning. However, they assume that there is no solvent in the asphaltene-rich phase. This assumption must be tested; however there is only limited data available in the literature for the measured composition of asphaltene-rich phase.

Chapter Three: Experimental

This chapter discusses the materials and methodologies used in this thesis. The experimental procedure adopted to determine the composition of solvent in the asphaltene-rich phase is described. The solubility and SARA fractionation data used in this thesis are taken from previously collected data by the same group. The details of these experimental procedures are explained elsewhere (Alboudwarej et al., 2002, Alboudwarej, 2003).

3.1 Materials

The experiments for determining the composition of the asphaltene-rich phase were conducted using Athabasca bitumen and asphaltene derived from Athabasca bitumen. Athabasca Coker feed bitumen was obtained from Syncrude Canada Ltd. It is the Syncrude Plant-7 froth treatment product after the solvent has been removed. Commercial grade toluene and n-heptane were obtained from Univar Canada and ConocoPhillips, respectively. n-pentane and n-decane were obtained from ConocoPhillips and Fisher Scientific, respectively and were 99.3% pure.

Asphaltenes were precipitated from the bitumen by the addition of either n-pentane or n-heptane at a 40:1 volume ratio of n-alkane to bitumen. The mixture was sonicated using an ultrasonic bath for 45 minutes and left overnight to settle. After settling, the supernatant was filtered through Whatman #2 (8μm) filter paper without disturbing the whole solution. At this point approximately 10% of the original mixture remained

unfiltered. The remaining precipitate was further diluted with the n-alkane at a 4:1 alkane:bitumen volume ratio. The mixture was sonicated for 45 minutes, left overnight and finally filtered using the same filter paper.

The precipitate was washed with the n-alkane until no discoloration was observed in the washings. The asphaltenes were dried in a vacuum oven at 50° C until no change in weight was observed. Asphaltenes precipitated with n-pentane and n-heptane are termed C5- and C7-asphaltenes, respectively.

3.2 Determination of the Solvent Content of the Asphaltene-Rich Phase

When a "good" solvent like toluene is added to solid asphaltenes, the asphaltene particles completely dissolve in the solvent. When a "poor" solvent like n-pentane or n-heptane is then added to this mixture, asphaltenes are precipitated. Similarly, in the case of bitumen diluted with n-alkane solvents, asphaltenes are precipitated. The resultant mixture separates into a light liquid phase, which is rich in solvents, and a heavy phase, which is rich in asphaltenes. The issue that arises is whether this heavy phase is a glassy liquid or a solid (Hirschberg, 1984, Kawanaka et al., 1991, Sirota, 2005, Gupta, 1986). In this work, this phase is treated as a liquid. For clarity, the two liquid phases will be called the solvent-rich phase and the asphaltene-rich phase, respectively. The objective of the proposed experiment is to determine the solvent content of the asphaltene-rich phase.

The asphaltene-rich phase manifests as a dispersed phase of particles, with diameters in the order of one micron, that form floccs of up to several hundred microns in diameter,

Figure 3-1 (Rastegari et al., 2004). The particles settle into a sediment layer and are surrounded by an entrained continuous phase (the solvent-rich phase). The remainder of the continuous phase forms a layer of free solvent above the sediment. It is required to measure the amount of solvent in the dispersed particles without including solvent from the continuous phase. In other words, the solvent in the asphaltene-rich phase must be clearly distinguished from the free and entrained solvent.

A methodology was designed to determine the mass of solvent in the asphaltene-rich phase only. The methodology is based on the rapid evaporation of the continuous phase solvent relative to the solvent dissolved in the asphaltene-rich phase. The free or entrained solvent evaporates directly while the solvent in the dense phase must first diffuse to the surface of the particle. Hence, there is an observable change in the evaporation rate when the entrained solvent finishes evaporating and only evaporation of solvent from the asphaltene-rich phase continues.

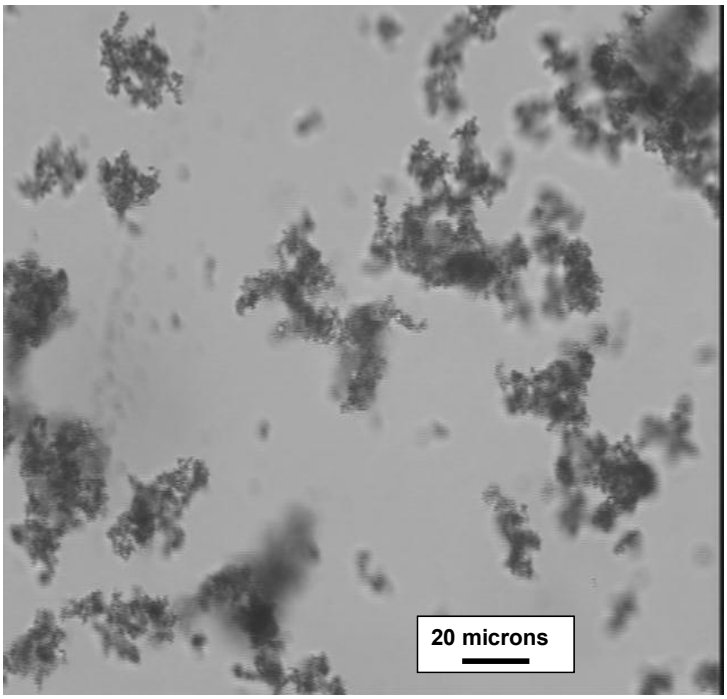

Figure 3-1: Micrograph of asphaltenes precipitated from a solution of asphaltenes in toluene and n-heptane (Rastegari, M.Sc. thesis, 2003).

3.2.1 Asphaltene and Solvent Systems

The methodology is illustrated in **Figure 3-2**. In Step 1, asphaltenes are first dissolved in toluene and sonicated for 30 minutes. A given volume of a poor solvent, such as an n-alkane, is then added to precipitate the asphaltenes. The amount of the poor solvent to be added is calculated based on the desired initial n-alkane volume fraction (Φ_H^o). The mixture is again sonicated for 30 minutes and left overnight to equilibrate. The mixture is then filtered using a Whatman filter paper #2. Part of the wet filter cake is placed in a Petri dish and more n-alkane solvent is added, if needed. The solvent is then allowed to

evaporate from the Petri dish in a nitrogen atmosphere. The mass of material in the Petri dish is measured over time until the mass is constant.

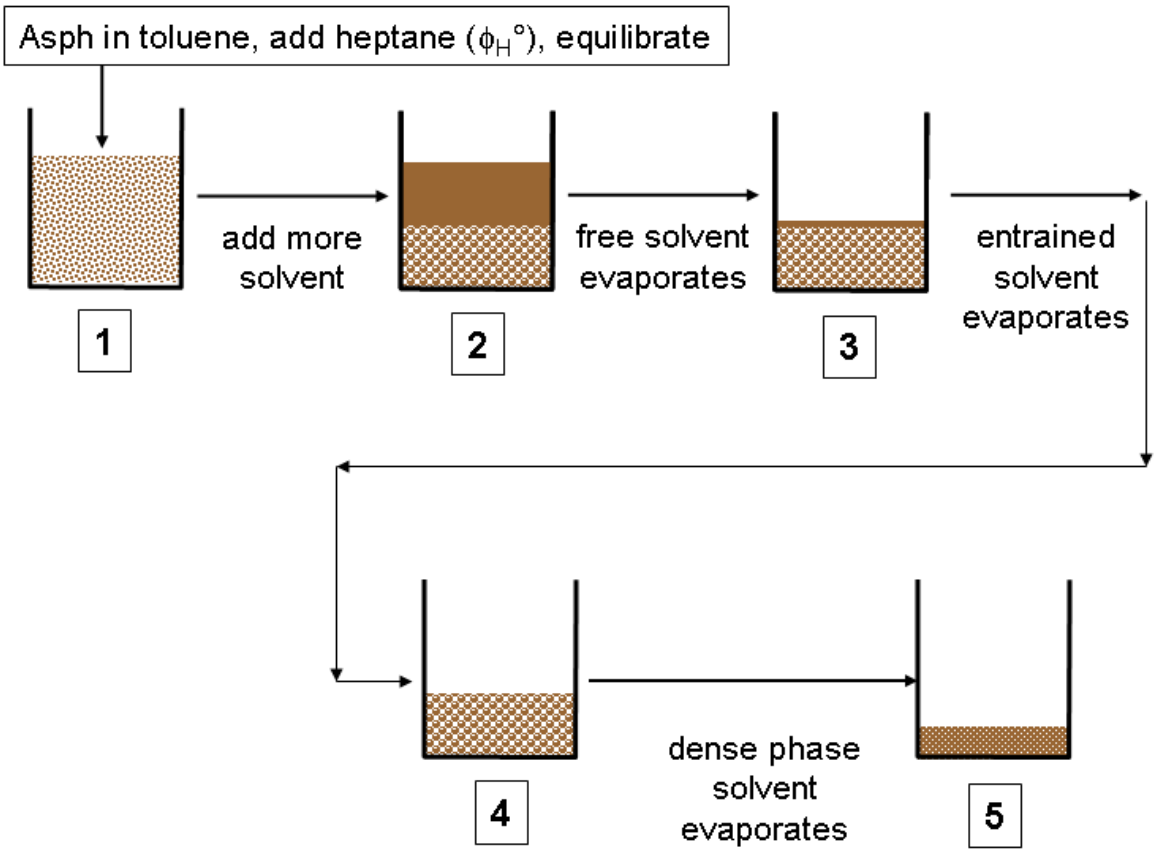

Figure 3-2: Experimental procedure to determine the solvent content of the asphaltene-rich phase.

In Step 2, the free solvent evaporates until only the entrained solvent and the asphaltene-rich phase remain. In Step 3, the entrained solvent evaporates until only the asphaltene-

rich phase remains. At Step 4, the solvent from the asphaltene-rich phase diffuses from the particles and evaporates until only dry asphaltenes remain at Step 5.

A hypothetical evaporation curve is shown in **Figure 3-3**. The amount of solvent in the asphaltene-rich phase is determined from the difference in mass between Step 4 and Step 5. The key to a successful experiment is a sharp transition from a rapid evaporation rate to a slow evaporation occurring at Step 4. In other words, all of the entrained solvent has evaporated before the solvent from the asphaltene-rich phase begins to evaporate.

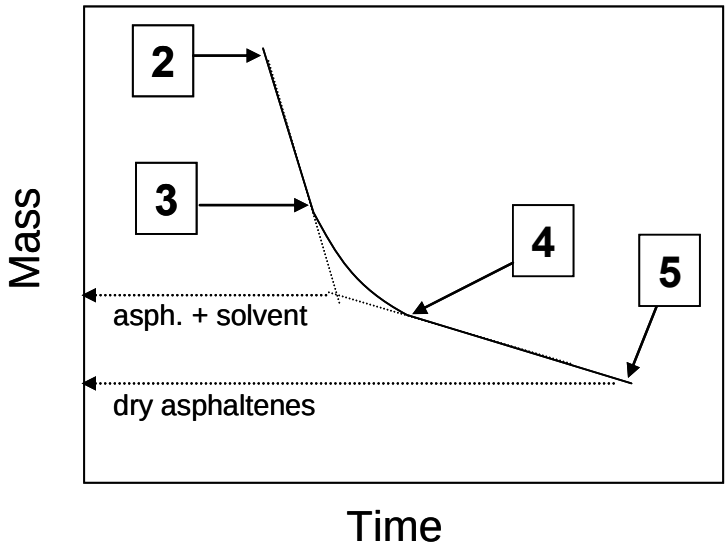

Figure 3-3: Vaporization curve of solvent from asphaltene/solvent mixture.

In reality, some of the solvent in the asphaltene-rich phase evaporates while the entrained solvent is evaporating. If the amount is relatively small, then there will be a sharp transition from Step 3 to Step 4. Otherwise, the evaporation curves for the free solvent

and for the asphaltene-rich phase solvent can be extrapolated, **Figure 3-3**. The point where they meet indicates the mass of the asphaltene-rich phase.

In all cases, the evaporation experiments were conducted in a bench top oven in a nitrogen atmosphere. An inert gas atmosphere like nitrogen is required to prevent the asphaltenes from oxidizing. The oven was maintained at a room temperature and pressure so that the solvent evaporation rates were the same in all experiments.

The experiment was repeated with different solvents (n-heptane, n-pentane and n-decane), asphaltene types (C5-asphaltenes and C7-asphaltenes), initial n-alkane volume fractions, and layer thicknesses of the asphaltene-rich phase in the Petri dish.

3.2.2 Diluted Bitumen Systems

In the case of bitumen, the above procedure for asphaltene-solvent systems was repeated with slight modifications. In Step 1, Bitumen was diluted with a poor solvent, such as n-heptane, at the desired dilution ratio. The mixture was sonicated for 45 minutes and left overnight to equilibrate. The mixture was then filtered using a Whatman filter paper #2. Part of the wet filter cake was placed in a Petri dish and more n-alkane solvent was added, if needed. From this point, Steps 1 to 5 were carried out as described previously. The experiment was repeated with different dilution ratios and layer thickness.

Note bitumen contains other constituents: saturates, aromatics, and resins. These constituents may also partition to the asphaltene-rich phase. These other constituents are

also present in the solvent-rich phase and are non-volatile. Therefore, they will not evaporate and will accumulate in the residue as the solvent evaporates. At the high dilutions used in these experiments, the potential error is 0.87%, as determined in Section 5.2.

3.3 Summary

An experimental procedure was developed to determine the solvent content of the asphaltene-rich phase. The methodology is based on the rapid evaporation of the free/entrained solvent relative to the solvent dissolved in the asphaltene-rich phase. As long as there is a sharp transition from a rapid evaporation rate of free/entrained solvent to a slow evaporation of solvent in the asphaltene-rich phase, the solvent content in the asphaltene-rich phase can be determined from the transition point. Procedures were developed for both asphaltene-solvent systems and diluted bitumen systems.

Chapter Four: Modeling

In this chapter, the theory and modeling methodology used in this research-project are presented. The modeling is based on a modification to regular solution theory and a brief description of the model and the details of the fluid characterization are presented. The determination of the molar mass, molar volume, and solubility parameter, which are required in the regular solution model, is explained. In the last section, the flash calculation procedure is discussed and a flow chart for the flash program is provided.

4.1 Modified Regular Solution Model

The separation of the fluid into a solvent-rich and an asphaltene-rich phase is modeled as a liquid-liquid equilibrium process. For two liquid phases at equilibrium, the fugacity of each component is identical in each phase:

$$f_i^{L1} = f_i^{L2} \qquad \textbf{(4-1)}$$

where f_i is the fugacity of component i, and $L1$ and $L2$ denote the two liquid phases. The fugacity of a component in liquid can be expressed as (Smithand van Ness, 1987),

$$f_i^{L} = x_i \gamma_i f_i^{0} \qquad \textbf{(4-2)}$$

where x_i, γ_i and $f_i°$ are the mole fraction, activity coefficient, and standard state fugacity, respectively. Eq. 4-2 is substituted into Eq. 4-1 to obtain:

$$x_i^{L1} \gamma_i^{L1} = x_i^{L2} \gamma_i^{L2} \qquad \textbf{(4-3)}$$

Eq. 4-3 provides the relationship between the composition of each phase which is required for phase equilibrium calculations. The relationship is usually expressed as an equilibrium ratio, K:

$$K_i = \frac{x_i^{L1}}{x_i^{L2}} = \frac{\gamma_i^{L2}}{\gamma_i^{L1}} \qquad \textbf{(4-4)}$$

Eqn. 4-4 shows that the equilibrium ratio for two liquid phases can be determined solely from the activity coefficients.

Several researchers have derived the activity coefficient for asphaltenes and crude oils based on regular solution theory (Hirschberg et al., 1984; Kawanaka et al., 1991; Yarranton and Masliyah, 1996). The model in this thesis is from Akbarzadeh et al. (2005) where the activity coefficient of a component in a given phase is based on regular solution theory (Scatchard, 1931; Hildebrand, 1929) modified with a Flory-Huggins entropy contribution (Flory, 1941; Huggins, 1941), and is given by:

$$\gamma_i = \exp\left(1 + \ln\frac{v_i}{v_m} - \frac{v_i}{v_m} + \frac{v_i}{RT}\left(\delta_i - \delta_m\right)^2\right) \qquad \textbf{(4-5)}$$

where R is the universal gas constant, T is temperature, v_i and δ_i are the molar volume and solubility parameter of component i, respectively and v_m and δ_m are the molar volume and solubility parameter of liquid phase, respectively. The second and third terms of the expression are the entropic contribution from different sized molecules and the final term is derived from the internal energy of mixing a regular solution. The model requires the molar volume and solubility parameter of each component in addition to the temperature, pressure and overall composition.

4.2 Fluid Characterization

The fluids in this work are solutions of asphaltenes in solvents or diluted bitumens. The solvent properties are known and were taken from the literature. The bitumen or heavy oil was divided in three pseudo-components (saturates, aromatics, and resins) as well as asphaltenes. The asphaltenes were treated as a mixture of nano-aggregates and were divided into pseudo-components representing different aggregate sizes. The composition of the fluid was determined from measured solvent and asphaltene or bitumen amounts and, when required, the SARA analysis of the bitumen.

4.2.1 Molar Mass

The molar masses of the solvents were obtained from the literature (NIST data) and listed in **Table 4-1**. The molar masses of the saturates, aromatics, and resins were measured directly.

Table 4-1: Molar mass of solvents (NIST data).

Component	Molar mass (g/mol)
n-pentane	72.2
n-hexane	86.2
n-heptane	100.2
n-octane	114.2
n-decane	142.3
n-toluene	92.1

The distribution of asphaltene nano-aggregates was divided into pseudo-components based on the gamma distribution function given by Equation 2-8.

For positive values of α, the gamma function can be written as:

$$\Gamma(\alpha) = \int_0^\infty t^{\alpha-1} e^{-t}\, dt \qquad \textbf{(4-6)}$$

The monomer molar mass was set to 1500 g/mol. Molar masses from vapour pressure osmometry extrapolate to a monomer molar mass of approximately 1800 g/mol, while high resolution mass spectrometry indicates monomer molar masses of approximately 1000 g/mol (Pinkston et al., 2009). The choice of 1500 g/mol is a compromise which can be revisited when the average monomer molar mass is better resolved. Yarranton et al. (2007) demonstrated that, while some retuning is required, the model is not very sensitive to the choice of monomer molar mass.

Asphaltene was divided into 30 sub-fractions with molar mass ranging up to 45000 g/mol. The average molar mass is an input for the model. For asphaltenes in solvents, the average molar mass of the aggregated asphaltenes is measured directly using vapour pressure osmometry (VPO). The value of α was determined by fine-tuning the model fit to precipitation data from solutions of asphaltenes in n-heptane and toluene. A value of 5 was found to fit the data. Once the distribution was set, the equations are solved numerically.

4.2.2 Densities and Molar Volumes

The densities of the solvents at 25°C were obtained from the VMGSim component database and listed in **Table 4-2**.

Table 4-2: Densities of solvents (VMGSim component database, VMGSim v5.0, 2009).

Component	Density (Kg/m^3)
n-pentane	630.5
n-hexane	656
n-heptane	682
n-octane	699
n-decane	728
n-toluene	865

The densities of saturates and aromatics were calculated using correlations taken from Akbarzadeh et al. (2005) model.

$$\rho_{sat} = 0.6379\mathrm{T} + 1069.54 \qquad \textbf{(4-7)}$$

$$\rho_{aro} = 0.5943\mathrm{T} + 1164.73 \qquad \textbf{(4-8)}$$

where ρ_{sat} and ρ_{aro} are densities of saturates and aromatics in kg/m³ respectively. T is the absolute temperature in K.

For resins and asphaltenes, the densities were correlated to the molar mass (Alboudwarej et al., 2003).

$$\rho = 670\ M^{0.0639} \qquad \textbf{(4-9)}$$

where ρ is the asphaltene density in kg/m³ and M is the molar mass in g/mol.

The molar volumes are simply the ratio of the molar mass to the density:

$$v_i = \frac{M_i}{\rho_i} \qquad \textbf{(4-10)}$$

where v_i, M_i and ρ_i are the molar mass and density of component i, respectively.

4.2.3 Solubility Parameters

Solubility parameters of the solvent were taken from Barton (1991), **Table 4-3**.

Table 4-3: Solubility parameters of components (Barton, 1991).

Components	**Solubility Parameter ($MPa^{1/2}$)**
n-pentane	14.3
n-hexane	14.8
n-heptane	15.2
n-octane	15.5
n-decane	15.8
toluene	18.2

Solubility parameters of saturates and aromatics were found using the following equation.

$$\delta_i = A_i + B_i T \qquad \textbf{(4-11)}$$

The values of A (in $MPa^{1/2}$) and B (in $MPa^{1/2}/K$) were found by fitting saturates/toluene/asphaltene and n-heptane/aromatics/asphaltene data, respectively, and are given in **Table 4-4**. The values of A and B used in the old model are also listed for comparison.

Table 4-4: Solubility parameters of saturates and aromatics.

Components		New Model	Old Model
Saturates	**A**	16.61	15.8
	B	0	0
Aromatics	**A**	18.5	20.3
	B	0	0

The solubility parameters of resins and asphaltenes were calculated using Equation 2-11. The value of *A(T)* is found by fitting the n-heptane/toluene/asphaltene data and is given by

$$A(T) = 0.00024\mathrm{T} + 0.2447 \qquad \textbf{(4-12)}$$

The value of A(T) is assumed to be the same for the resins. Since A(T) increases with temperature and the asphaltene density is assumed to be invariant with temperature, the solubility parameter of the asphaltenes is predicted to increase with temperature. However, this trend is physically incorrect because the solubility parameter is proportional to the square root of the internal energy of vaporization which decreases with temperature. The discrepancy is likely an artefact arising because the solubility parameters of the other components were held constant where in fact they also decrease with temperature. This incorrect temperature dependence will not alter the conclusions of this work because it is the difference between the solubility parameters that is significant. Nonetheless, the error will be corrected in future work to obtain a physically correct form of the solubility parameter correlation.

4.3 Flash Calculations

The flash program presented here is based on an iterated equilibrium ratio (K-value) update with damping. In the inner loop of the program, the Rachford-Rice equations are solved using a bounded Newton-Raphson method. In the outer loop, the outer K-values are updated with damping.

4.3.1 Inner Loop

The Rachford-Rice equation (Rachford and Rice, 1952), which is used to solve the liquid-liquid equilibrium calculations, is given by:

$$\sum_i^n \left(x_i^{L1} - x_i^{L2}\right) = \sum_i^n \frac{z_i\left(K_i - 1\right)}{1 + \left(K_i - 1\right)\beta} = 0 \qquad \textbf{(4-13)}$$

In this application, the values of z_i and K_i are known and the equation is solved for β, which is the fraction of solvent rich phase. K_i is the liquid-liquid equilibrium ratio.

Based on the minimum and maximum values of K-value of components, the left and right boundaries of β are calculated.

$$\mathrm{LB} = \frac{1}{(1 - \mathrm{K}_{\max})} \qquad \textbf{(4-14)}$$

$$\mathrm{RB} = \frac{1}{(1 - \mathrm{K}_{\min})} \qquad \textbf{(4-15)}$$

where LB and RB are the left and right boundary of β.

The Rachford-Rice equation is non-linear and the equation above is solved using the Newton-Raphson (NR) method.

$$\beta_{n+1} = \beta_n - \frac{P(\beta_n)}{P'(\beta_n)} \qquad \textbf{(4-16)}$$

where $P(\beta_n)$ is the Rachford-Rice function and $P'(\beta_n)$ is its derivative with respect to β. $P(\beta_n)$ and $P'(\beta_n)$ are given by the following equations.

$$P(\beta) = \sum_i \frac{z_i(K_i - 1)}{1 + (K_i - 1)\beta} \qquad \textbf{(4-17)}$$

$$P'(\beta) = -\sum_i \frac{z_i(K_i - 1)^2}{(1 + (K_i - 1)\beta)^2} \qquad \textbf{(4-18)}$$

The initial estimated value for β is 0. The initial values of *K* are estimated for each component. The function is iterated until the change in the value of β per iteration is below a given threshold, in this case, be 10^{-16}. If the value calculated is outside the left and right boundaries, the value of β is modified as follows:

$$\beta_{n+1} = 0.5(\beta_n - LB) \qquad \text{if } \beta < LB \qquad \textbf{(4-19)}$$

$$\beta_{n+1} = \beta_n + 0.5(RB - \beta_n) \qquad \text{if } \beta > RB \qquad \textbf{(4-20)}$$

where β_{n+1} is the new β value and β_n is the β value from the previous iteration. β is the current β value, LB and RB are the left and right boundaries of β.

Once the value of β is converged, the compositions of solvent-rich phase and asphaltene-rich phase are calculated using the following equations.

$$x_i^{L1} = \frac{K_i z_i}{\beta(K_i - 1) + 1} \quad \textbf{(4-21)}$$

$$x_i^{L2} = \frac{z_i}{\beta(K_i - 1) + 1} \quad \textbf{(4-22)}$$

where, in this application, x_i^{L1} and x_i^{L2} are the mole fractions of component *i* in the solvent-rich phase and the asphaltene-rich phase, respectively.

4.3.2 Outer Loop

The activity coefficients and equilibrium ratios are recalculated based on the updated compositions from the inner loop. The equilibrium ratios are modified with a damping factor as follows:

$$K_i^{new} = \exp\left\{\ln K_i^{prev} + DF * \left(\ln K_i^{curr} - \ln K_i^{prev}\right)\right\} \quad \textbf{(4-23)}$$

where *DF* is the damping factor, K_i^{new} is the new value of *K*, K_i^{curr} is the current value of *K* calculated using equation 4-4 and K_i^{prev} is the value of K at the previous iteration. A value of damping factor of 0.15 – 0.4 is used in this work to improve the convergence.

The difference between the values of β at the current iteration and previous iteration and the difference between the values of K_i for each component at the current iteration and previous iteration are used to calculate the overall error.

$$\varepsilon = \beta^{err} + K^{err} \quad \textbf{(4-24)}$$

$$\beta^{err} = \left[\beta^{prev} - \beta^{curr}\right]^2 \quad \textbf{(4-25)}$$

$$K^{err} = \sum_i \left[K_i^{curr} - K_i^{prev}\right]^2 \quad \textbf{(4-26)}$$

where ε is the overall error, β^{err} is the error from vapour fraction and K^{err} is the total error from K-values of each component. β^{curr} is the current value of β and β^{prev} is the value of β at the previous iteration.

The outer loop is iterated until the overall error is less than the tolerance value of 10^{-12}.

All the calculations are performed in Microsoft Excel, using the Visual Basic for Applications (VBA) coding interface. A flow chart showing the calculation procedure is given in **Figure 4-1**.

4.4 Summary

An existing regular solution model was modified to allow all components in the asphaltene-rich phase to take part in the phase equilibrium. A flash program was developed which used iterated equilibrium ratio updating with damping. The Rachford-Rice equations were solved using a bounded Newton-Raphson method. The model was re-tuned using n-heptane/toluene/ asphaltene precipitation data.

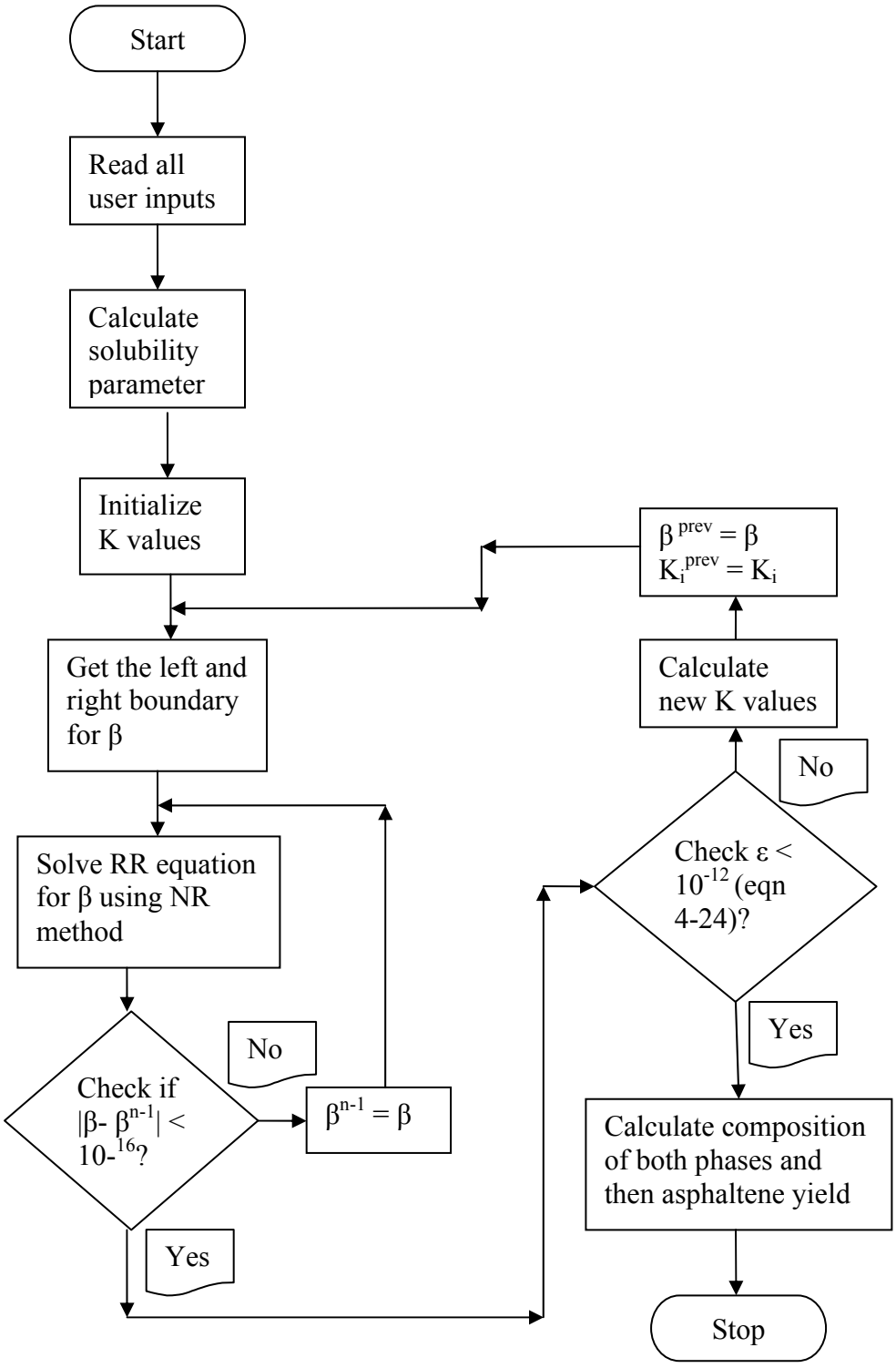

Figure 4-1: Flow chart for the calculation of asphaltene precipitation.

Chapter Five: Measurement of Asphaltene-Rich Phase Compositions

The methodology to determine phase compositions from the evaporation experiments is validated. The solvent contents of the asphaltene-rich phases from asphaltene/solvent systems are discussed including the effect of the type of solvent and asphaltenes. The extension of the method to n-heptane diluted bitumen is also presented.

5.1 Asphaltene-Rich Phases from Asphaltene/Solvent Systems

5.1.1 Validation of Method

As explained in Chapter Three:, the amount of solvent in an asphaltene-rich phase was determined from an evaporation experiment. The accuracy of the measurement depends on a distinct transition from free and entrained solvent evaporation to diffusive evaporation from the asphaltene-rich phase, **Figure 3-3**. In particular, if the evaporation of the entrained solvent is slower than the evaporation of free solvent above the sediment, the beginning of diffusive evaporation from the asphaltene-rich phase may be undetectable.

To test the effect of the entrained solvent evaporation rate, experiments were performed with different thicknesses of sediment. In a thin sediment layer, the volume of entrained solvent is small and the exposed surface area is large; hence, evaporation is expected to continue at the same rate as the free solvent. In thick layers, there may be sufficient entrained solvent at the bottom of the sediment layer that some diffusive evaporation occurs from the top of the sediment before all of the entrained solvent has evaporated.

Figure 5-1 shows the normalized solvent evaporation rate (normalized mass of solvent versus time) for an evaporation experiment performed on a sediment obtained from a mixture of 10 g/L asphaltenes in a solution of toluene and n-heptane with an initial heptane volume fraction of 0.5. The thickness of the layer was calculated to be approximately 15 microns based on the measured dry mass of the asphaltenes, an asphaltene density of 1180 kg/m^3, and area of the Petri dish. The normalized solvent mass was computed by dividing the measured mass of solvent at any time with the initial solvent mass.

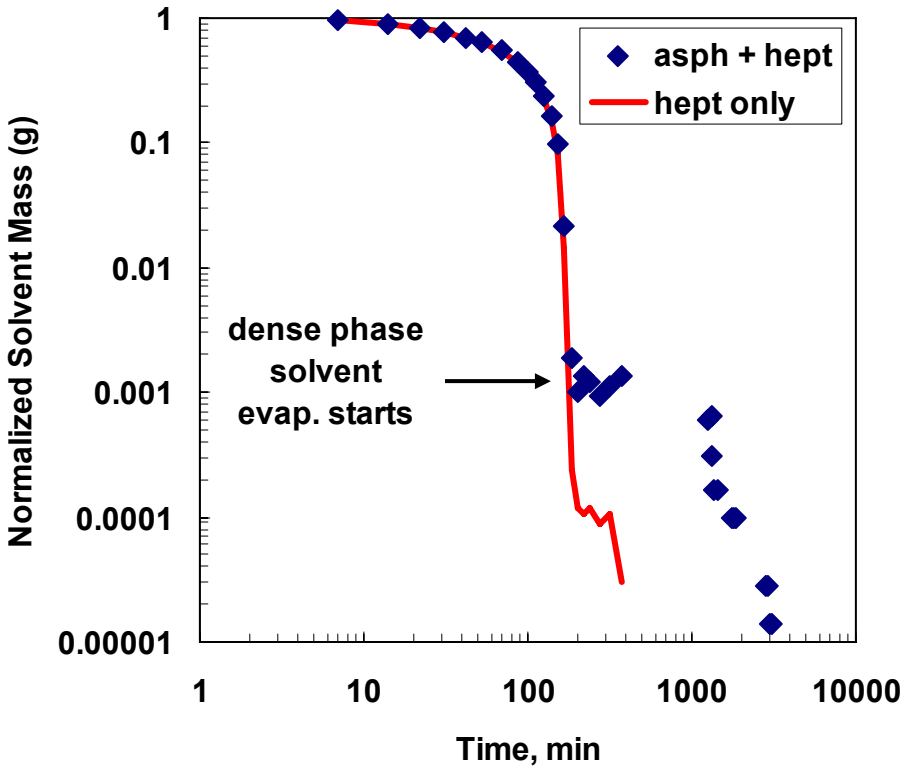

Figure 5-1: Evaporation curve from very thin asphaltene sediment obtained from 10 g/L asphaltenes in solution of 50 vol% toluene and 50 vol% n-heptane at 23° and atmospheric pressure.

The normalized rate of solvent evaporation from the asphaltene-solvent system is compared with that of pure n-heptane in **Figure 5-1**. The evaporation rates are identical while the free solvent evaporates and a sharp transition to a much slower evaporation rate is observed at a normalized solvent mass of approximately 0.001. There appears to be a second transition to a more rapid evaporation rate at a normalized solvent mass of approximately 0.0008. This second transition is an artefact from using a log scale to plot the data.

To determine the solvent content in the asphaltene-rich phase, the transition from solvent-free evaporation to diffusive evaporation was found as follows:

- Data points that are clearly on the entrained solvent evaporation line were selected and extrapolated using a regressed power equation.
- Data points that are clearly on the diffusive evaporation line were selected and extrapolated using a regressed power equation.
- The intersection point of the two fitted equations was determined and this is the point where the evaporation transitions from entrained solvent evaporation to diffusive evaporation.

The above steps are illustrated in **Figure 5-2** for an asphaltene/heptane/toluene system. The solid symbols are diffusive evaporation data and the open symbols are the entrained solvent evaporation data. The precision of the measurement is determined by calculating the deviation between the observed transition point and the calculated transition point.

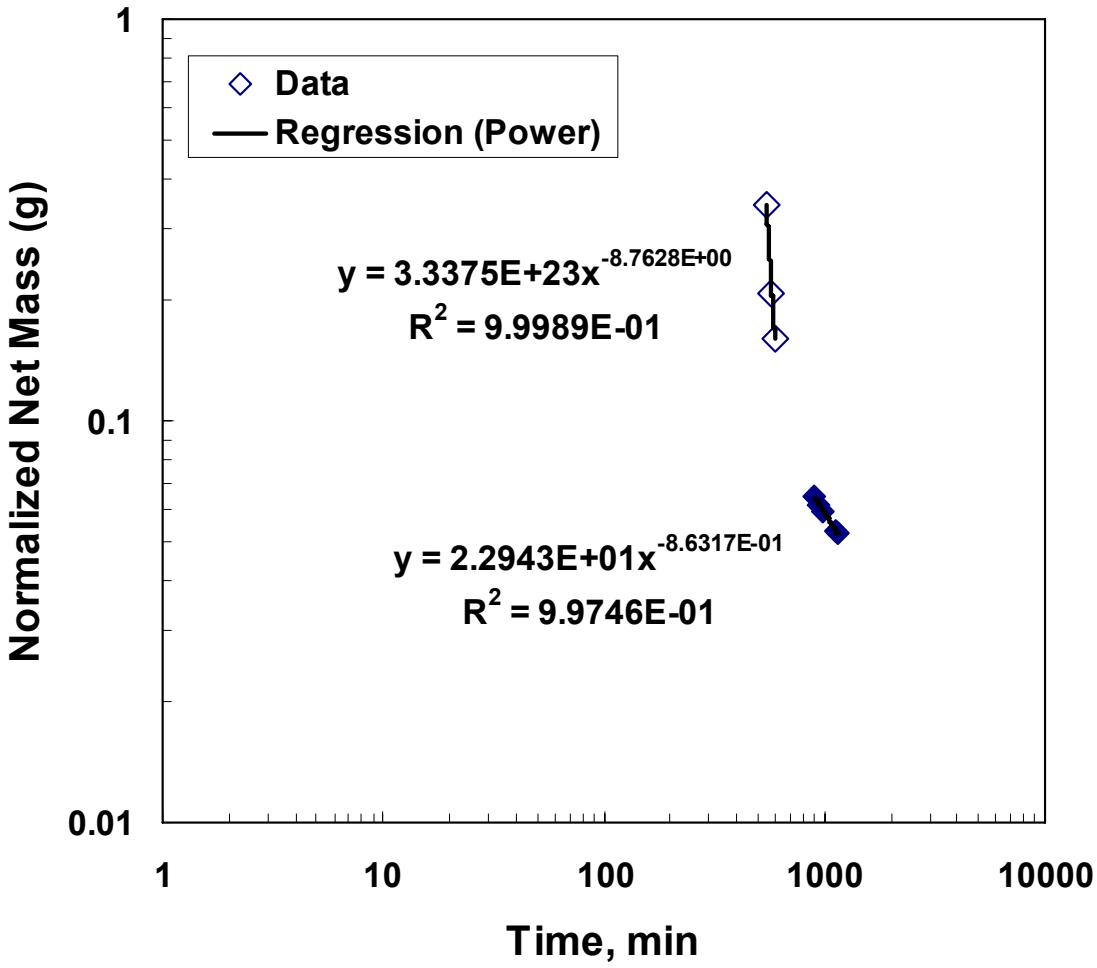

Figure 5-2: Calculation of Precision for asphaltene-rich phase composition experiments.

For the data presented in **Figure 5-2**, the transition point was determined to occur at a normalized solvent mass of 0.0073, corresponding to a solvent content of 6 ±2%. The sharpness of the transition from rapid to slow evaporation and the low value of the determined solvent content both indicate that the entrained solvent evaporated at the same rate as the free solvent and that the procedure correctly identified the beginning of

diffusive evaporation. Note, ±2% indicates the precision of the measurement. The repeatability of the measurement will be discussed later.

The previous experiment was performed on a very thin sediment and the accuracy of the results is limited by the accuracy of the mass determination for the very small mass of asphaltenes (0.1178 g). Therefore, the experiments were repeated for thicker layers. **Figure 5-3** compares the normalized evaporation rates from "thin" and "thick" sediments obtained from mixtures of asphaltene in n-heptane and toluene. The initial solution was prepared with a heptane volume fraction of 0.65. The thickness of the thick layer is 3-5 mm and that of thin layer is 0.18 mm.

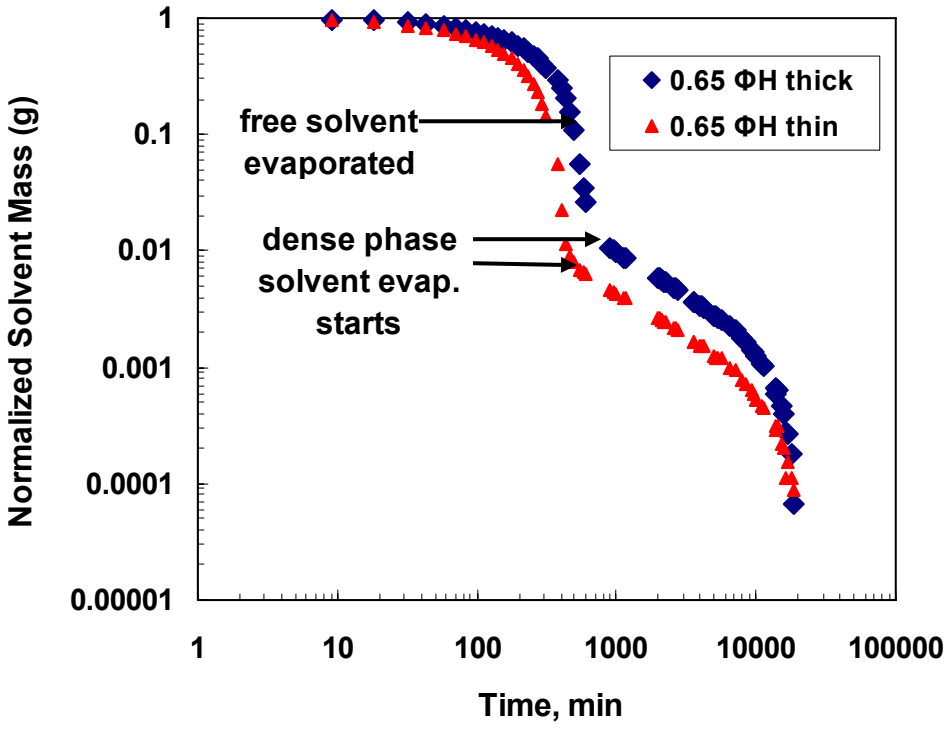

Figure 5-3: Effect of thickness of sediment on transition to diffusive evaporation from asphaltene sediment. Sediment obtained from 10 g/L asphaltenes in solution of 65 vol% -n-heptane and 35 vol% toluene at 23° and atmospheric pressure.

In both cases, a sharp transition from rapid to slow evaporation is observed. The solvent contents in the asphaltene-rich phase for the thick and thin layers were 7 ±2% and 6.9 ±0.5%wt%, respectively. Similar results were obtained for all of the experiments performed on sediments obtained from solution of asphaltenes, toluene, and n-alkanes, **Table 5-1**. The sharp transitions and the consistency of the solvent contents confirm that the entrained solvent evaporates at the same rate as the free solvent and does not effect the determination of the onset of diffusive evaporation.

Table 5-1: Solvent compositions of asphaltene-rich phases obtained from solutions of 10 g/L asphaltenes in toluene and an n-alkane at 23°C and atmospheric pressure.

Solvent (Init. n-alk. Vol. Fr)	***Asph type* (layer)***	***Mass percent of Solvent***
n-heptane (0.50)	C7 (thin)	6 ± 1
n-heptane (0.50)	C7 (thick)	5.9 ± 0.7
n-heptane (0.65)	C7 (thin)	6.9 ± 0.5
n-heptane (0.65)	C7 (thick)	7 ± 2
n-heptane (0.80)	C7 (thin)	7.2 ± 0.6
n-heptane (0.80)	C7 (thick)	6.2 ± 0.5
n-pentane (0.80)	C7 (thin)	5.3 ± 0.3
n-pentane (0.80)	C7 (thick)	6.5 ± 0.2
n-decane (0.80)	C7 (thin)	5.1 ± 0.5
n-decane (0.80)	C7 (thick)	7.1 ± 0.1
n-heptane (0.80)	C5 (thin)	5.4 ± 0.1
n-heptane (0.80)	C5 (thick)	5.8 ± 0.5

* All asphaltenes were separated from Athabasca bitumen

5.1.2 Sediment from Solutions of Asphaltenes in Solvents

The effect of initial n-alkane volume fractions, solvents and asphaltene types on the composition of asphaltene-rich phase are studied in this section. The choice of n-alkane solvents and its initial composition are expected to have an effect on the phase behaviour

and may affect the composition of the solvent in the asphaltene-rich phase. The experiments were conducted with C5 and C7 asphaltenes to see the effect of asphaltene types on the composition of asphaltene-rich phase. C7-asphaltenes is more representative of "pure" asphaltenes because less resins are co-precipitated with them than with the C5-asphaltenes (Agrawala and Yarranton, 2001; Yarranton et al., 2000).

Initial n-Alkane Volume Fraction

Figure 5-4 compares the results of the experiments performed on asphaltene/n-heptane/toluene mixture with initial heptane volume fraction of 0.65 and 0.80. The solvent contents in the asphaltene-rich phase were 7 ±2 and 6.2 ± 0.5 wt% for the initial heptane volume fraction of 0.65 and 0.8, respectively. The solvent content for the sediment from a solution with an initial n-heptane volume fraction of 0.50 was 5.9 wt%, **Table 5-1**. The solvent contents are the same within the precision of the measurements. Hence, there is no evidence that the solvent content of the asphaltene-rich phase is sensitive to the volume fraction of heptane in the solution from which the sediment is precipitated.

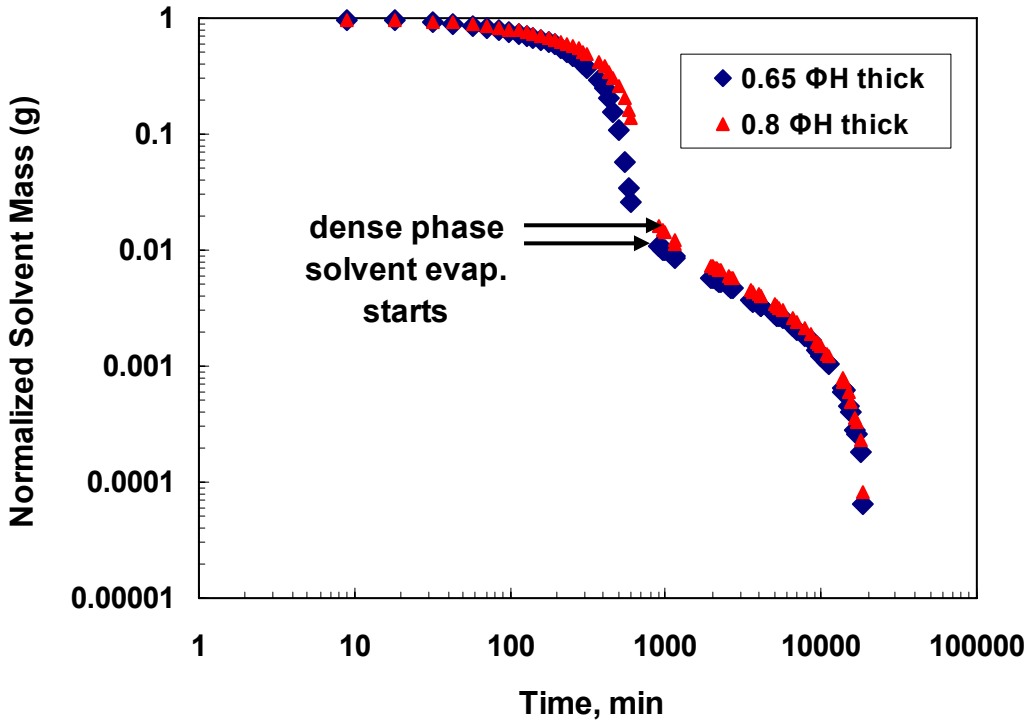

Figure 5-4: Evaporation curves for sediments obtained from sediments obtained from 10 g/L asphaltene in solutions of n-heptane and toluene with different initial n-heptane volume fractions at 23°C and atmospheric pressure.

Asphaltene Type

The experiments in the preceding sections were performed using asphaltenes extracted using n-heptane (C7-asphaltenes). The experiments with an initial heptane volume fraction of 0.8 were repeated with C5-asphaltenes, **Figure 5-5**. The solvent contents in the asphaltene-rich phase for the thick and thin layers were 5.8 ±0.5 and 5.4 ±0.1 wt%, respectively. The results with C5-asphaltenes appear to be within the precision of the results of C7-asphaltenes. So the choice of asphaltenes does not affect the composition of solvent in the asphaltene-rich phase.

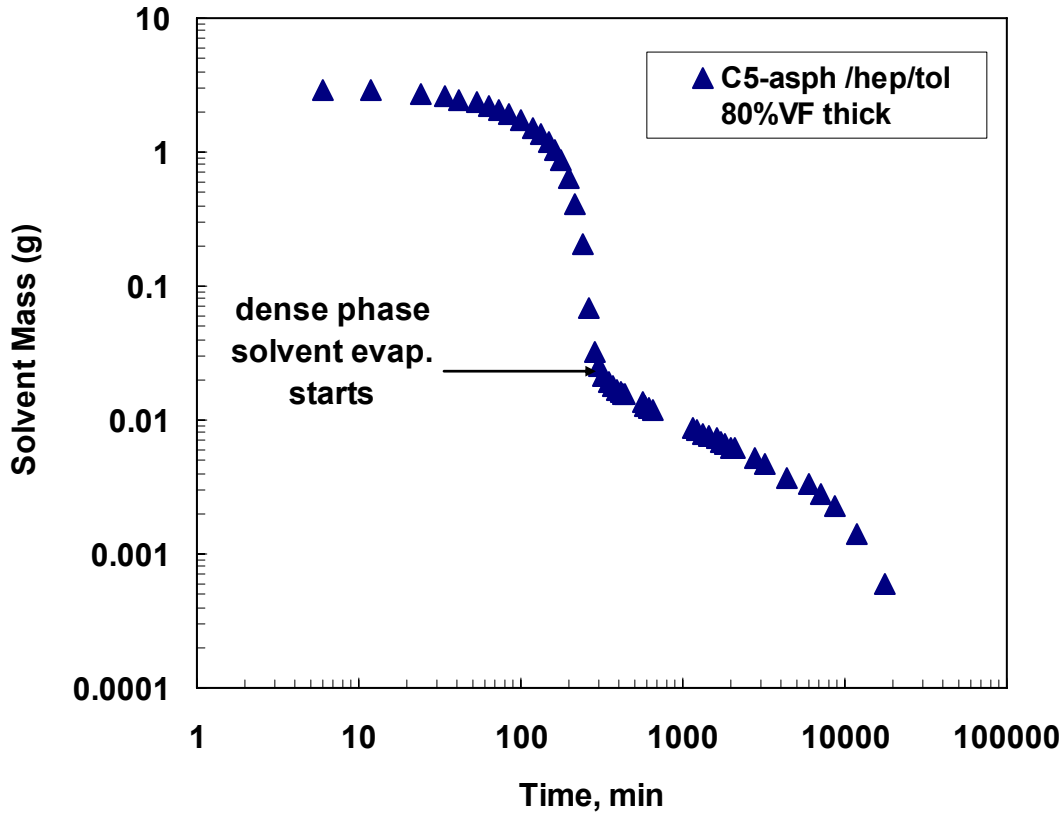

Figure 5-5: Composition of solvent in the asphaltene-rich phase of C5-asphaltene/ heptane/toluene system.

Solvent Type

The evaporation experiments were performed using n-pentane and n-decane instead of n-heptane. **Figure 5-6** shows the results for the asphaltene/n-pentane/toluene system with an initial pentane volume fraction of 0.80. **Figure 5-7** shows the results for the asphaltene/n-decane/toluene system. Note the relatively rapid evaporation rate with n-pentane and the slow evaporation rate with n-decane both for the free solvent and with diffusive evaporation.

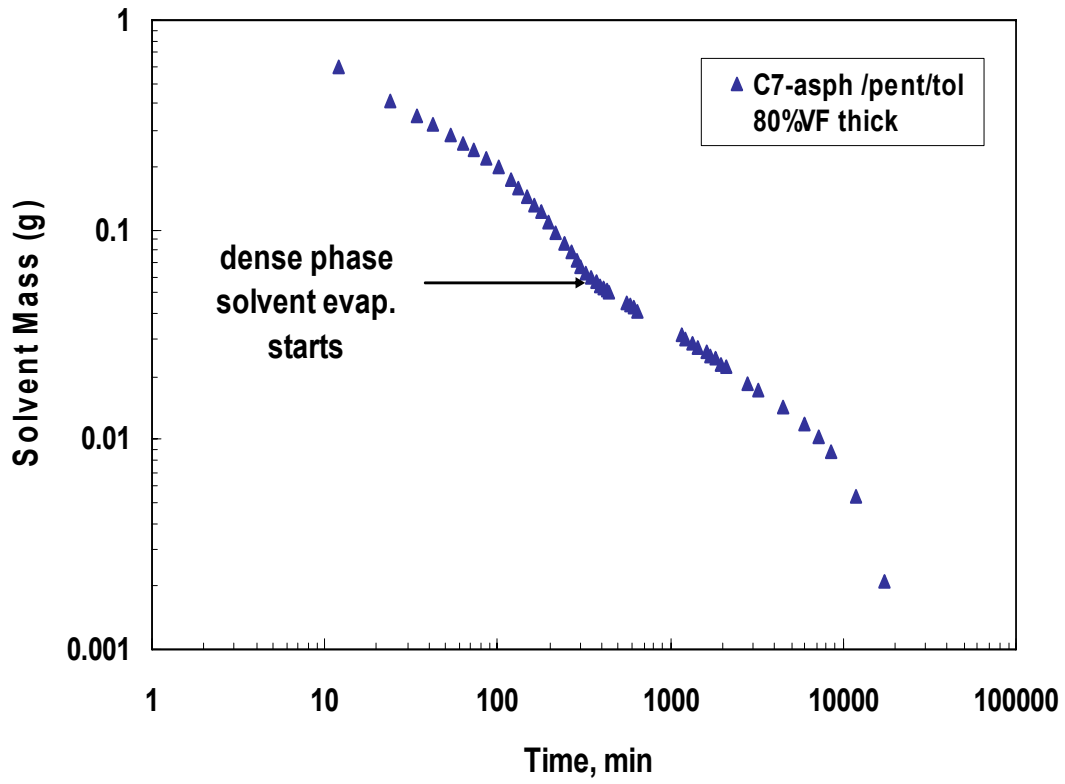

Figure 5-6: Composition of solvent in the asphaltene-rich phase of C7-asphaltene/n-pentane/ toluene system.

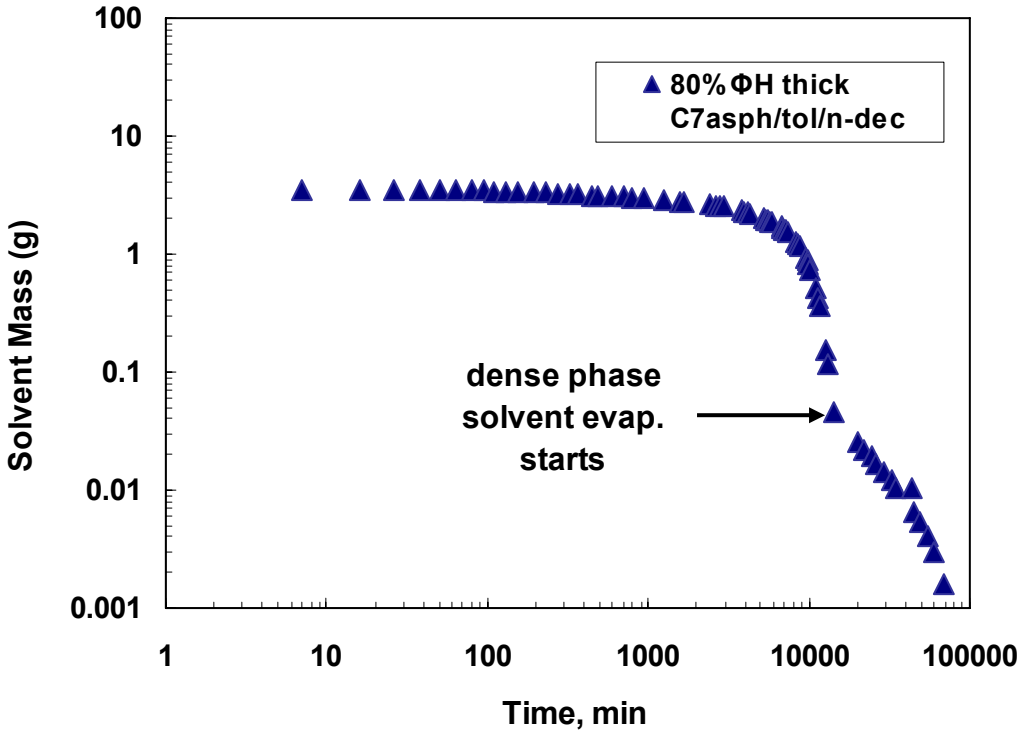

Figure 5-7: Composition of solvent in the asphaltene-rich phase of C7-asphaltene/n-decane/toluene system.

The solvent contents in the asphaltene-rich phase for the asphaltene/n-alkane/toluene systems were as follows:

n-pentane	6.5 ±0.2 wt% (thick layer) and 5.3 ±0.3 wt% (thin layer)
n-heptane	6.2 ±0.5 wt% (thick) and 7.2 ±0.6 wt% (thin)
n-decane	7.1 ±0.1 wt% (thick) and 5.1 ±0.5 wt% (thin)

Note, the given ranges for the above data indicate the precision of the measurement. Repeatability tests were performed and the solvent content was found to be repeatable to within ±0.9% based on a 95% confidence interval (details provided in the Appendix).

The weight percent of solvent in the asphaltene-rich phase for asphaltene/solvent systems is then 6.1 ± 0.9 %.

5.2 Asphaltene-Rich Phases from Solvent Diluted Bitumen

The same methodology was applied to sediments obtained from bitumen diluted with n-heptane. The analysis is more complicated because bitumen contains non-asphaltene constituents (saturates, aromatics, and resins) which are non-volatile. These components may partition to the asphaltene-rich phase during the initial precipitation. They will also be part of the solvent phase and will remain in the sediment after the solvent evaporates.

The mass of saturates, aromatics, and resins in the solution can be determined from the known mass of bitumen and solvent. Assuming that all of these components are present only in the solvent phase, the maximum mass of these components in the solvent phase transferred to the Petri dish for an evaporation experiment corresponds to a percent error of approximately 0.87% in the mass of asphaltene. Therefore the presence of saturates, aromatics and resins leads to an overestimation of 0.87% on the weight of asphaltene in the asphaltene-rich phase. Of more concern is the effect of these components on the evaporation rate of the solvent.

Figure 5-8 shows the evaporation profile for a “thick” sediment obtained from a 40:1 g heptane/g bitumen. The transition from free and entrained solvent evaporation to diffusive evaporation from the dense phase is not as pronounced for the diluted bitumen compared with the asphaltene/solvent systems. The same method was used to determine a

transition point from the intersection of the extrapolated entrained solvent evaporation data and the extrapolated diffusive evaporation data. In this case, the solvent content in the asphaltene-rich phase was 9 ± 1 wt%.

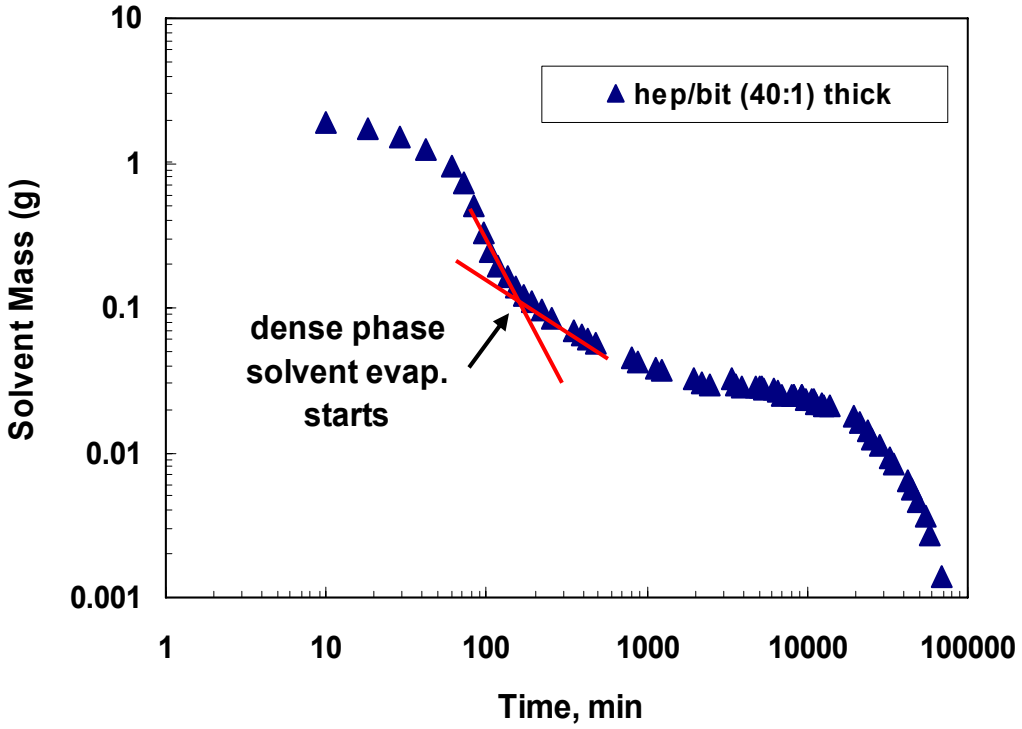

Figure 5-8: Composition of solvent in the asphaltene-rich phase of diluted bitumen.

Table 5-2 summarizes the solvent content of the asphaltene-rich phases from n-heptane diluted bitumen. The results indicate that the weight percent of solvent in the asphaltene-rich phase of diluted bitumen is 11 ± 4 %. The dilution ratio and the thickness of the asphaltene-rich phase particles do not appear to affect the composition of solvent in the

asphaltene-rich phase, within the precision of the experiment. The data shows more variability that the asphaltene-solvent results.

Table 5-2: Summary of solvent content of asphaltene-rich phases obtained from n-heptane diluted bitumen at 23°C and atmospheric pressure

Heptane dilution (g/g)	***Mass percent of solvent***
1.9 (thick)	12.1 ± 0.3
1.9 (thin)	5.6 ± 0.3
4.0 (thin)	10.3 ± 0.7
4.0 (thick)	14.7 ± 0.1
40.0 (thin)	15.5 ± 0.5
40.0 (thick)	11 ± 1
40.0 (thick-no additional solvent*)	9.3 ± 0.6
40.0 (thick-no additional solvent*)	9 ± 1

* - No additional solvent added to the Petri dish before the start of the experiment.

Note, the given ranges for the above data indicate the precision of the measurement. Repeatability tests were performed and the solvent content was found to be repeatable to within ±4.1% based on a 95% confidence interval (details provided in the Appendix). The weight percent of solvent in the asphaltene-rich phase for diluted bitumen systems is then 11 ± 4 %.

5.3 Summary

The amount of solvent in an asphaltene-rich phase was determined from the developed evaporation experiment. The experimental methodology was tested by using a thin sediment layer where the volume of entrained solvent is small. For the asphaltene-solvent system, the effect of the initial n-alkane volume fractions, asphaltene types and solvents on the composition of asphaltene-rich phase is studied. The solvent content of the asphaltene-rich phase was found to be insensitive to the volume fraction of n-alkane, solvent or asphaltene type. The composition of solvent in the asphaltene-rich phase was found to be 6.1 ± 0.9 wt%.

The composition experiments for diluted bitumen system were performed using n-heptane. It was found that the n-heptane dilution ratio did not affect the composition of solvent in the asphaltene-rich phase, within the precision of the experiment. The data obtained were more scattered than those from the asphaltene/solvent data. The weight percent of solvent in the asphaltene-rich phase of diluted bitumen was 11 ± 4%.

Chapter Six: Modeling Amount and Composition of Asphaltene-Rich Phases

The modified regular solution model is tested on asphaltene precipitation data from the literature and the composition data from Chapter 5. The ability of the model to predict the effect of different solvents, temperatures, asphaltene source, and asphaltene molar mass is evaluated. The model predictions are also compared with prediction from the old model with no solvent-partitioning to identify how the model predictions changed.

The data for fractional precipitation of asphaltene by solutions of n-heptane solvent and toluene at different temperatures was obtained from Akbarzadeh et al., 2005 (Figure 6-1). The washing procedure data and other crude oil data were taken from Alboudwarej et al., 2002 (Figure 6-2, Figure 6-3 and Figure 6-4). The fractional precipitation of asphaltene by solutions of n-alkane solvent and toluene was obtained from Yarranton et al., 1996 and Mannistu et al., 1997 (Figure 6-6 and Figure 6-7). The concentration of asphaltene is 10 g/L, unless otherwise specified. Note the average absolute deviation (AAD) for each data set is given in the appendix.

6.1 Retuning the Model

The first step in modeling was to retune the asphaltene solubility parameters by fitting asphaltene yields from 10 g/L asphaltenes in n-heptane and toluene at 0, 23, and 50°C, **Figure 6-1**. The correlation for the asphaltene solubility parameter used in the old model (no solvent partitioning) is given by:

$$A(T) = 0.579 - 0.00075\mathrm{T} \qquad \textbf{(6-1)}$$

and the retuned correlation is given by:

$$A(T) = 0.2447 + 0.00024\mathrm{T} \qquad \textbf{(6-2)}$$

In the old model, the value of shape factor of the gamma distribution function α was found using a temperature dependent correlation.

$$\alpha = 10.177963 - 0.025926\mathrm{T} \qquad \textbf{(6-3)}$$

For example, the value of α is 2.5 at 23 ^{o}C. It was found that no temperature correction was required for shape factor with the new model as the retuned *A* correlation could capture the temperature dependence. The value of α was set to 5. With these minor modifications, the new model fitted the yield data within the error of the measurements.

Figure 6-1a and **Figure 6-1b** shows the fitted precipitation data for Athabasca asphaltene in solutions of n-heptane and toluene for the new model and old model respectively. The AAD for the new model at 0 °C, 23 °C and 50 °C were 0.0315, 0.0422 and 0.0254, respectively. The deviations are slightly greater than obtained with the old model (AAD at 0 °C, 23 °C and 50 °C were 0.0238, 0.0218 and 0.0137, respectively).

After the model was retuned, the parameters were fixed and it is no longer a fitting model but a predictive model for asphaltene/solvent systems. The only input required is the average molar mass of asphaltenes, which is a value typically measured for each asphaltene type. Next, the effectiveness of the new model was assessed by its capability to predict the effect of solvent type, asphaltene type, and asphaltene molar mass.

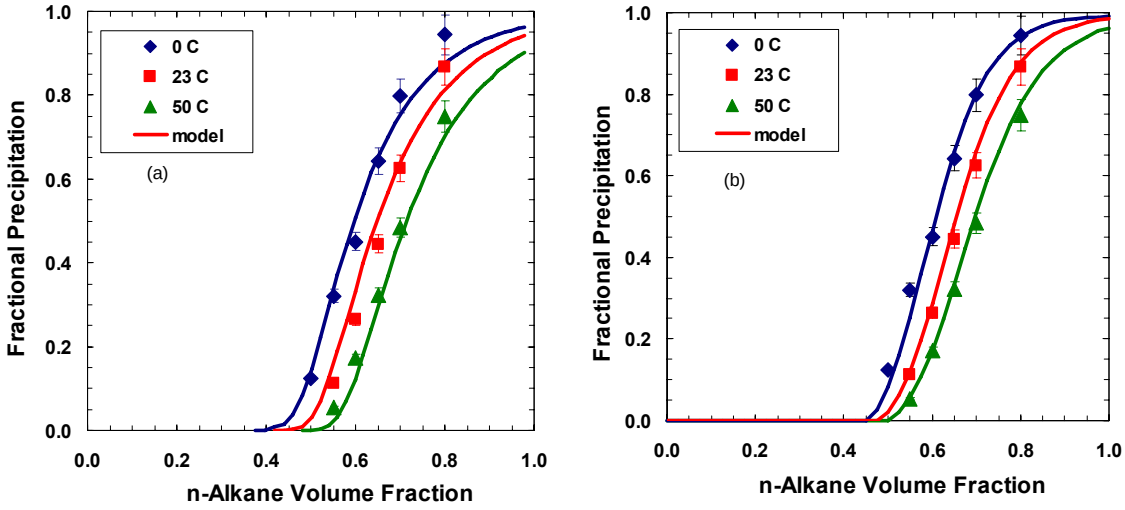

Figure 6-1: Effect of temperature on precipitation from solutions of 10 g/L Athabasca asphaltenes in solutions of n-heptane and toluene (a) New model (b) Old model (Data from Akbarzadeh et al., 2005)

6.1.1 Effect of Asphaltene Molar Mass – Washing Effect

Recall that asphaltenes are self-associated and the average molar mass is the molar mass of the aggregated asphaltenes. Asphaltenes that are washed more extensively have on average a higher molar mass, **Table 4-3**. Asphaltene precipitation increases as the average asphaltene molar mass increases. The yield predictions for the washed asphaltenes are presented in **Figure 6-2a** for the new model and in **Figure 6-2b** for the old model with no solvent partitioning.

Figure 6-2 shows that both models under-predict the fractional precipitation for the Soxhlet-washed asphaltenes. Note, the amount of precipitation increases for higher molar mass material. Given the variability and limited accuracy of VPO measurements

(Alboudwarej et al, 2003), it is likely that the measured average associated asphaltene molar masses are lower than the actual molar masses. The average molar mass could be adjusted to better fit the data but that was not the purpose of this work.

The old model provides good predictions for the Sonicator-washed and Unwashed asphaltenes. The new model provides a similar prediction for the Sonicator washed asphaltenes but under-predicts the yield for the low molar mass Unwashed asphaltenes. **Table 6-2** gives the predictions of solvent content in the asphaltene-rich phase from the new model. The new model significantly over-predicts the amount of solvent in the low molar mass asphaltenes which leads to an under-prediction of the fractional precipitation. The effect of the solvent content is discussed in more detail later in Section 6.1.5.

The average absolute deviations for the new model were 0.1123, 0.1048 and 0.0568 for fractional precipitation of unwashed, sonicator-washed and soxhlet-washed asphaltenes with solvent, respectively. For the old model, the AAD were 0.0166, 0.1102 and 0.0979 for fractional precipitation of unwashed, sonicator-washed and soxhlet-washed asphaltenes with solvent, respectively.

Table 6-1: Average molar masses of asphaltene with different asphaltene washing procedures (Data from Alboudwarej et al., 2002)

Washing Procedure	Av. Molar mass (g/gmol)
Unwashed	5700
Sonicator	7600
Soxhlet washed	9100

Table 6-2: Predicted solvent content of asphaltene-rich phase predicted by the model for washed Athabasca asphaltenes in solvents (n-heptane volume fraction: 0.8)

Washing Procedure	Composition of solvent (wt%)
Unwashed	41.5
Sonicator	36.8
Soxhlet washed	33.9

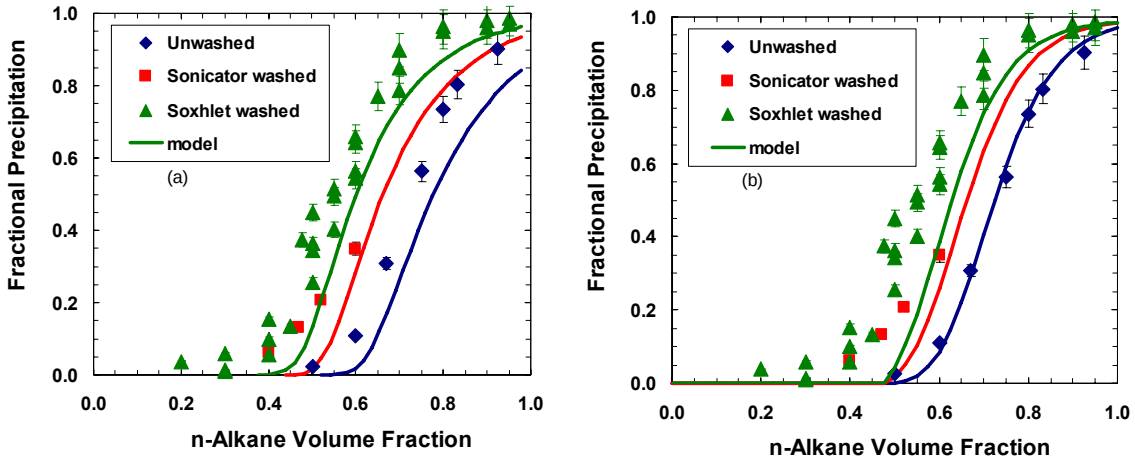

Figure 6-2: Effect of average asphaltene molar mass on precipitation of Athabasca asphaltenes from solutions of n-heptane and toluene at 23°C. (a) New model (b) Old model (Data from Alboudwarej et al., 2002).

6.1.2 Effect of Asphaltene Molar Mass - Asphaltene Source

The described experiments in **Figure 6-1** and **Figure 6-2** use asphaltenes derived from Athabasca bitumen. Data was also available for asphaltenes extracted from other heavy oils and bitumens including an Indonesian crude oil, two Venezuela heavy oils, a Russian heavy oil, and Cold Lake bitumen from Alberta. The average molar mass of these asphaltenes are given in **Table 6-3**. **Figure 6-3a** and **Figure 6-3b** show the fractional yields from solutions of these asphaltenes in n-heptane and toluene at 23°C for the new model and old model, respectively. The data and model results for Cold Lake and Indonesia asphaltenes are presented separately in **Figure 6-4** to avoid overcrowding of the data.

Figure 6-3 and **Figure 6-4** show that fractional precipitation for the asphaltenes from different sources as predicted by both the models. For the new model, the AAD values were 0.0413, 0.0466, 0.0638, 0.0680 and 0.2384 for Venezuela1, Venezuela2, Russia, Cold Lake and Indonesia asphaltenes with solvent, respectively. Note, Indonesia asphaltenes had a very low molar mass so the deviations in the new model predictions observed were similar to the Unwashed asphaltenes. The higher solvent content predicted in the asphaltene-rich phase for the low molar mass asphaltenes causes the fractional precipitation to be less than the actual precipitation.

Table 6-3: Average molar masses of different asphaltene types (Data from Alboudwarej et al., 2002)

Asphaltene types	Av. Molar mass (g/gmol)
Venezuela 1	10000
Venezuela 2	7700
Russia	7100
Cold Lake	7900
Indonesia	4600

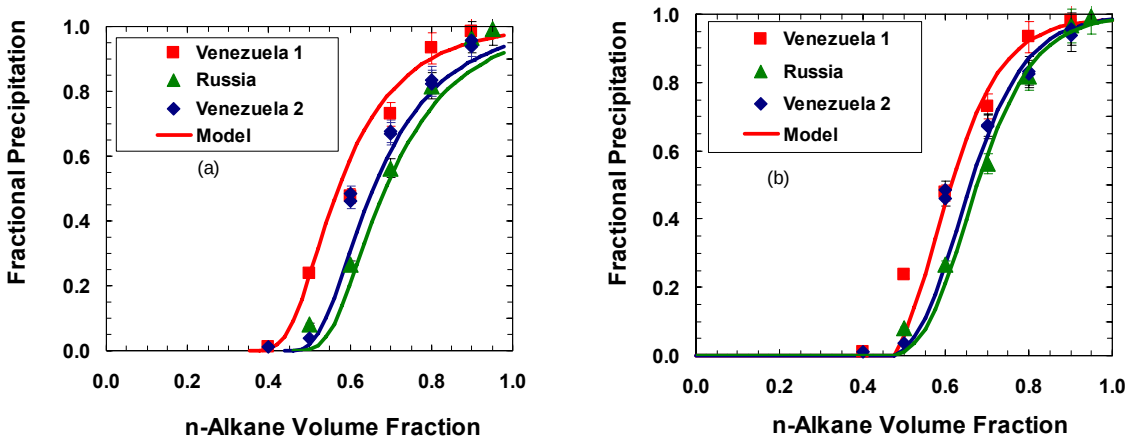

Figure 6-3: Effect of asphaltene source on precipitation from solutions of n-heptane and toluene at 23°C. (a) New model (b) Old model. (Data from Alboudwarej et al., 2002)

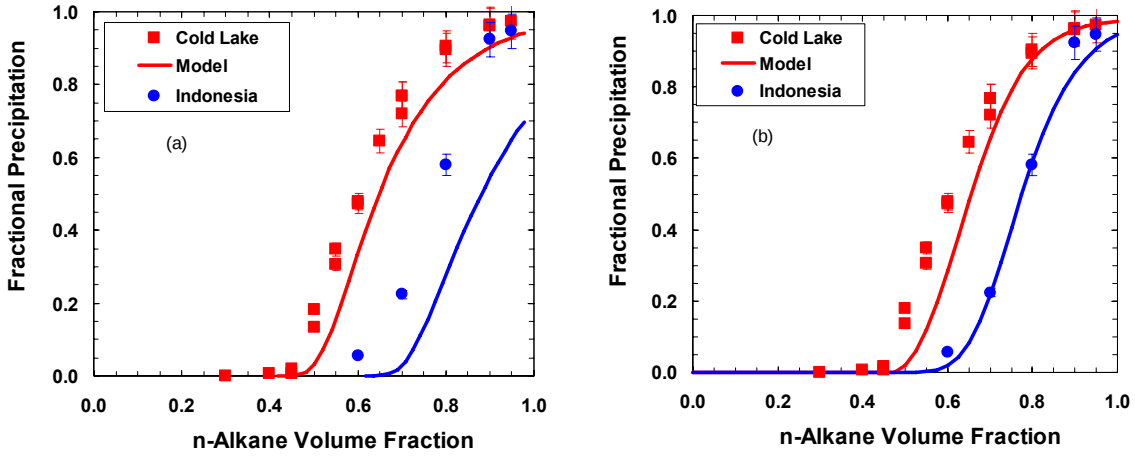

Figure 6-4: Fractional precipitation from n-alkane/toluene/asphaltenes (Cold Lake and Indonesia) mixture at 23°C. (a) New model (b) Old model (Data from Alboudwarej et al., 2002)

6.1.3 Effect of Asphaltene Concentration

The results presented so far are for asphaltene concentrations of 10 g/L. The model prediction of fractional precipitation of asphaltene at different asphaltene concentrations are given in **Figure 6-5**. The experimental data presented in **Figure 6-5** was taken from Yarranton and Masliyah (1996) but has been corrected to a solids-free basis based on a "solids" content of 6.3 wt% of the asphaltenes.

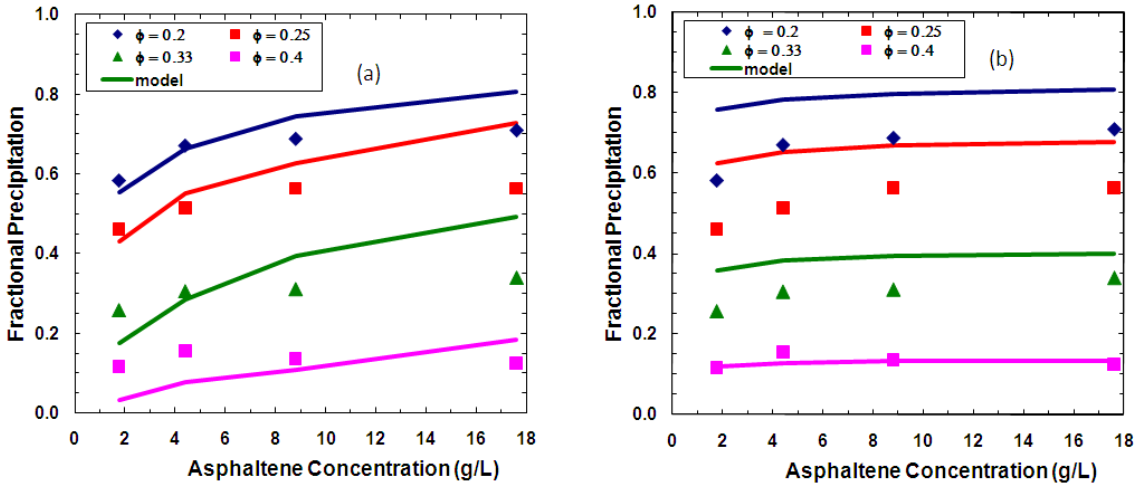

Figure 6-5: Fractional precipitation as a function of asphaltene concentration at different toluene volume fractions in hexane/toluene/asphaltene system. (a) New model (b) Old model (Data from Yarranton and Masliyah, 1996)

Figure 6-5b shows that the old model correctly predicts the low dependence of asphaltene fractional precipitation on asphaltene concentration especially at high concentrations of asphaltenes. The new model, **Figure 6-5a**, over-predicts the effect of dilution. However, it provides a better match to the data at low asphaltene concentrations. For the new model, the AAD values were 0.0469, 0.0735, 0.0851 and 0.0625 for toluene volume fractions of 0.20, 0.25, 0.33 and 0.4, respectively. The AAD values for the old model were 0.1249, 0.1304, 0.0803 and 0.0101 for toluene volume fractions of 0.20, 0.25, 0.33 and 0.4, respectively. The composition of solvent in the asphaltene-rich phase at different asphaltene concentrations and solvent volume fractions are given in **Table 6-4**.

Table 6-4: Predicted solvent content (wt%) of the asphaltene-rich phase at different asphaltene concentrations and toluene volume fractions

	Toluene Volume fraction			
asph conc (g/L)	**0.2**	**0.25**	**0.33**	**0.4**
1.76	37.89	42.08	48.99	52.61
4.4	39.01	43.57	51.37	55.96
8.8	39.76	45.09	53.68	59.06
17.6	40.32	46.46	55.94	62.49

6.1.4 Effect of Solvent Type

The model predictions of asphaltene fractional precipitation at 23°C from solutions of toluene with n-pentane, n-hexane, or n-heptane are shown in **Figure 6-6a** and from solutions of toluene with n-octane, n-decane in **Figure 6-7a**. Predictions using the old model (no solvent partitioning) for the same data are shown in **Figure 6-6b** and **Figure 6-7b**. As the carbon number of the n-alkane solvent increases up to approximately C8, the solubility of asphaltene also increases.

Since prediction of the effect of solvent requires only the solvent properties to be changed keeping constant all the asphaltene properties, this is a significant test of the predictive capability of the new model. While the old model predicts the effect of solvent within the scatter of the data, the model with solvent partitioning over-predicts the fractional

precipitation for n-pentane and under-predicts the fractional precipitation for n-octane and n-decane. The AAD for both the models is calculated in the Appendix.

Table 6-5 tabulates the composition of solvent in the asphaltene-rich phase for different solvents. The solvent content with n-pentane solvent is relatively lower than that of n-heptane and this explains why the asphaltene precipitation from that solvent is over-predicted. However, it can be seen that the solvent composition predicted with n-heptane and n-decane solvents are nearly equal. A possible explanation is that the retuned asphaltene solubility parameter was incorrect because the solvent content was incorrect. The effect of different n-alkanes depends on the difference in the solubility parameter between the solvents and asphaltenes. Therefore an incorrect asphaltene solubility parameter would adversely affect the predictions.

Figure 6-7 shows that the old model predicts the asphaltene precipitation to be almost the same for n-octane and n-decane. However, the data shows that the fractional precipitation is lower for n-decane than n-octane at high n-alkane volume fractions. The new model correctly predicts this difference in asphaltene precipitation at higher volume fraction. However, it is not sure if the difference in asphaltene precipitation at higher volume fraction is real or simply due to the scatter in the data.

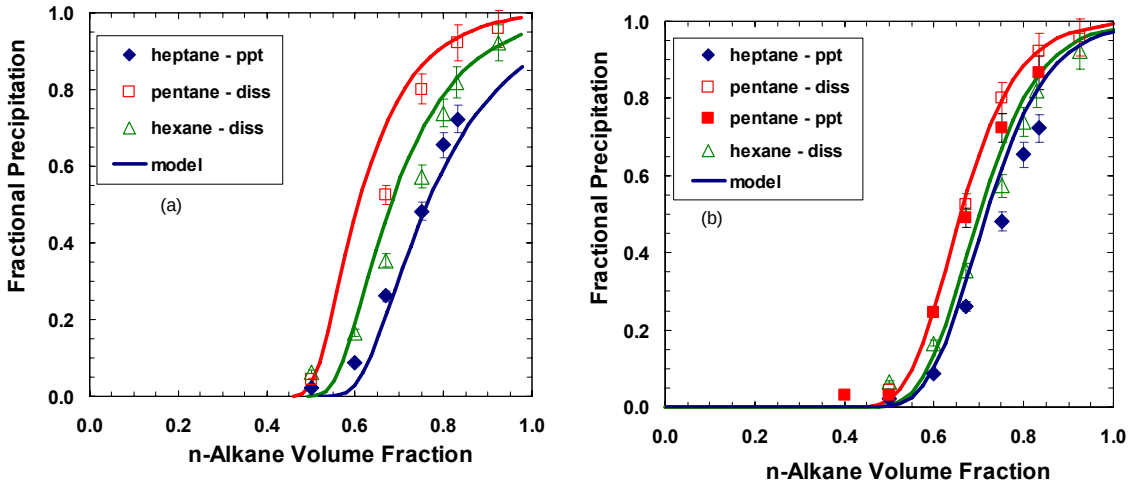

Figure 6-6: Fractional precipitation of Athabasca asphaltene at 23°C with different solvents. (a) New model (b) Old model (Data from Yarranton et al., 1996 and Mannistu et al., 1997)

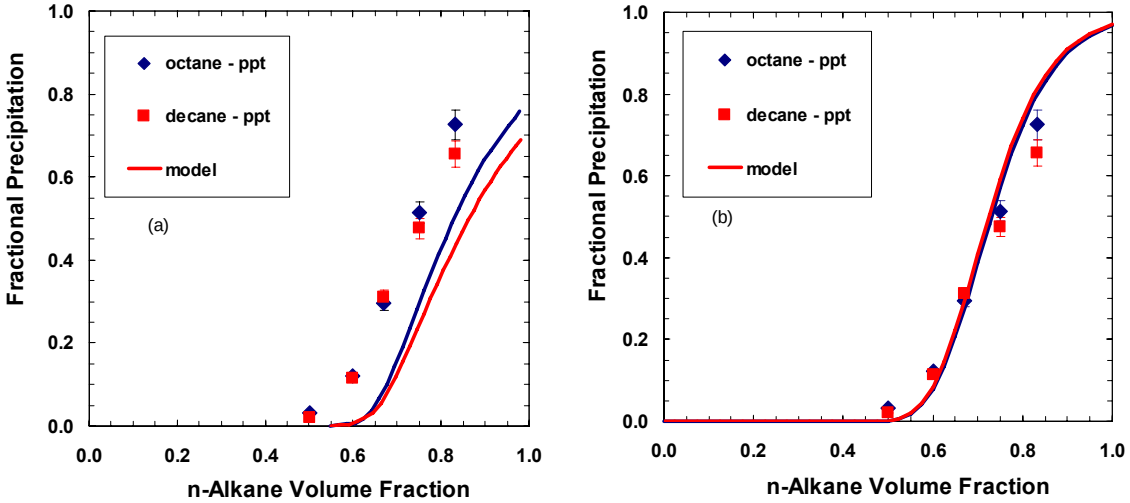

Figure 6-7: Fractional precipitation of asphaltene at 23°C with n-octane and n-decane solvents. (a) New model (b) Old model (Data from Yarranton et al., 1996 and Mannistu et al., 1997)

Table 6-5: Composition of solvent in the asphaltene-rich phase of n-alkane/ toluene/ asphaltenes (Athabasca) system for initial n-alkane volume fraction of 0.8.

Solvent	Wt% from experiment	Wt% from model
n-heptane	6.2	40.98
n-pentane	5.9	34.16
n-hexane	-	37.97
n-octane	-	42.25
n-decane	6.1	40.64

6.1.5 Solvent Content of the Asphaltene-Rich Phase

Figure 6-8 shows the predicted solvent content of asphaltene-rich phases for 10 g/L of 5900 g/mol asphaltenes in solutions of toluene and n-pentane, n-heptane, or n-decane. The predictions are from the new model, as the old model is constrained to have zero solvent in the asphaltene-rich phase. **Table 6-5** compares the measured and predicted solvent content in the asphaltene-rich phase for solutions of 0.8 volume fraction of an n-alkane and toluene. The model significantly over-predicts the solvent content.

In other words, when the model was tuned using n-heptane/toluene/asphaltene data, the tuning was based on an incorrect value of approximately 40 wt% for the solvent content versus the experimental value of 6.2 wt%. Therefore, the tuned asphaltene solubility parameter is incorrect. Both the incorrect solvent content and the incorrect solubility parameter could lead to poor predictions of asphaltene precipitation. An interaction

parameter may be needed to force the model to predict the solvent composition and fractional precipitation correctly.

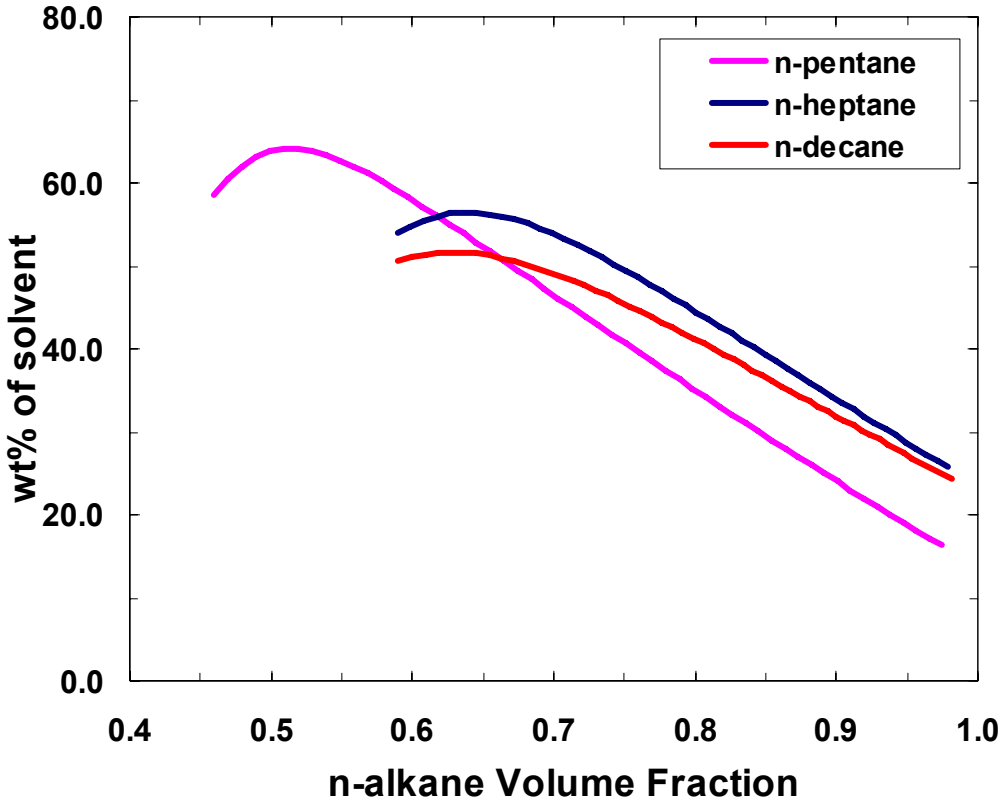

Figure 6-8: Weight percent of solvent as a function of n-alkane volume fraction

6.2 Summary

The new model was successfully retuned to fit the n-heptane/toluene/Athabasca asphaltene data. The new model predicted the effect of molar mass with approximately the same AAD as the old model except for the low molar mass asphaltenes. However, the model predicted a significant increase in fractional precipitation at higher asphaltene concentrations which was not observed experimentally. The predictions for different n-

alkanes were also poor. It is hypothesised that the poor predictions of fractional precipitation result from an over-prediction of the solvent content of the asphaltene-rich phase. The new model predicted solvent contents in the order of 35 to 40 wt% compared to measured values of approximately 6 wt%. It is recommended that a binary interaction parameter be used to correct the predicted solvent contents and then determine if the other prediction errors are corrected.

Chapter Seven: Conclusions and Recommendations

The objectives of this research were to develop an experimental procedure to determine the composition of solvent in the asphaltene-rich phase and to model asphaltene precipitation with all the components partitioning to all phases. This chapter presents the conclusions of this work and recommendations for future work.

7.1 Conclusions

7.1.1 Experimental

A methodology was developed to measure the composition of solvent in the asphaltene-rich phase. The experiments were based on the difference between the evaporation rate of the free or entrained solvent versus that of the solvent dissolved in the asphaltene-rich phase. The mass of a mixture of asphaltenes and solvent was measured over time and an evaporation curve was constructed.

As expected, it was observed that the entrained solvent evaporates much more rapidly than solvent in dense phase. In the case of n-alkane/toluene/asphaltene system, there was a clear and consistent change in slope when the entrained solvent evaporation ended. The amount of solvent in the asphaltene-rich phase was determined at this point. The experiments were performed on thick and thin layers of asphaltene particles. The effects of using different initial n-alkane volume fraction, asphaltene types and solvents were also studied. The amount of solvent in the asphaltene-rich phase was found to be 6.1 ±

0.9 wt%. The effect of initial n-alkane volume fraction, asphaltene types and solvents was within the precision of measurement.

In the case of diluted bitumen system, the transition from free solvent evaporation to diffusive evaporation was less pronounced. Hence, the measurement was less precise for the diluted bitumen system. A regression based technique was used to find the deviation point in this case. The results were more scattered and therefore the repeatability of the experiment decreased in comparison to asphaltene/n-alkane/toluene system. The amount of solvent in the dense phase was determined to be 11 ± 4 wt%.

7.1.2 Modeling

A previously developed regular solution model was adapted to allow all components to partition to each of the liquid phases. The fluids were characterized based on the previous study. The phase equilibrium calculations assumed liquid-liquid equilibrium. The flash program was based on an iterated equilibrium ratio (K-value) update with damping. The Rachford-Rice equations were solved using a bounded Newton-Raphson method. The parameters of the model were adjusted to get a good fit with n-heptane/toluene/ asphaltene precipitation data. Once the initial tuning was completed, the model parameters were fixed and the model became completely predictive.

The model predicted the fractional precipitation of asphaltenes with moderate to high average asphaltene molar mass (>7000 g/mol) fairly well. However, the predictions for low average molar mass asphaltenes were poor because the amount of solvent in the

asphaltene-rich phase was over-predicted. The predictions for other n-alkane solvents were also poor particularly n-octane and n-decane. Note, the old model handled the effect of solvents including the heavy solvents, well. The model did not predict the effect of asphaltene concentration well, at high asphaltene concentrations. The new model significantly over-predicts the solvent content of the asphaltene-rich phase. It would appear that the poorer performance of the new model is due to the over-prediction of the solvent content. Improving the solvent content issue may fix the problems related to yield prediction.

7.2 Recommendations for Future Work

The present experimental work could be extended to study the effect of temperature and other industrial solvents such as naphtha and gas oils. The present experimental procedure may need to be improved for these multi-component diluents.

The current experimental procedure measures the composition of the entire solvent; that is, the combined n-alkane and toluene amount for an n-alkane/toluene/asphaltenes experiment. A better methodology would be to find the individual composition of heptane and toluene. This data would be more valuable for tuning the model.

SARA analysis could be performed on the asphaltene-rich phase to determine the amount of saturates, aromatics, and resins in this phase. With these values, a more accurate picture of composition of asphaltene-rich phase could be obtained for the diluted bitumen experiments.

The model prediction of the solvent content of the asphaltene-rich phase is not accurate. A binary interaction parameter could be introduced into the regular solution model to tune the model to match the measured solvent composition. However, this option eliminates the simplicity of the current version of regular solution model, one of its key advantages.

An alternative approach may be to use an equation-of-state approach to predict the yield and composition of the asphaltene-rich phase. Hypothetical critical properties of asphaltene may be used to tune the Peng-Robinson 'a' and 'b' parameters. The binary interaction parameters could be adjusted to tune the composition of asphaltene-rich phase.

Another modeling approach is to combine both Peng-Robinson equation of state with regular solution model using an advanced mixing rule such as an excess Gibb's energy mixing rules. The advantage of this approach is that the liquid phase properties can be properly modeled within an equation of state framework. The Wong-Sandler mixing rule (Wong and Sandler, 1992) can be used for this purpose. The Wong Sandler mixing rule is derived by equating the Helmholtz free energies from two models at infinite pressure and assuming that Helmholtz free energy is a weak function of pressure. Also at low temperatures, the excess volume (V^E) is usually very small. Therefore,

$$A_{\gamma}^{E}(T,P=\infty,x_i) \approx A_{\gamma}^{E}(T,P=low,x_i) = G_{\gamma}^{E}(T,P=low,x_i) - PV^{E}(T,P=low,x_{,})$$

$$\approx G_{\gamma}^{E}(T,P=low,x_i) \qquad \textbf{(7-1)}$$

This leads to,

$$\frac{A_{\infty}^{E}(x)}{RT} = \frac{G^{E}(x)}{RT} \qquad \textbf{(7-2)}$$

where $A_{\infty}^{E}(x)$ is the Helmholtz free energy at infinite pressure and $G^{E}(x)$ is the Gibb's free energy at low pressure. R is the universal gas constant and T is the absolute temperature. The Helmholtz free energy calculated by the Peng-Robinson equation of state is matched with the excess Gibb's free energy calculated using regular solution theory. The Peng-Robinson EoS binary interaction parameters would be adjusted to match the free energies.

References

Agrawala, M., Yarranton, H.W., “Asphaltene Association Model Analogous to Linear Polymerization”, Ind. Eng. Chem. Res. 2001, 40, 4664-4672.

Akbarzadeh K., Alboudwarej, H., Svrcek, W.Y., Yarranton, H.W., “A generalized regular solution model for asphaltene precipitation from n-alkane diluted heavy oils and bitumens”, Fluid Phase Equilibria, 2005, 232, 159–170.

Alboudwarej, H., Svrcek, W.Y., Kantzas, A., Yarranton, H.W., "A Pipe Loop Apparatus to Investigate Asphaltene Deposition," J. Petr. Sci. Technol., 2004, 22(7&8), 799-820.

Alboudwarej, H., Beck, J., Svrcek, W. Y., Yarranton, H. W. and Akbarzadeh, K., “Sensitivity of Asphaltene Properties to Separation Techniques” Energy and Fuels, 2002, 16(2), 462-469.

Alboudwarej, H., Akbarzadeh, K., Beck, J., Svrcek, W.Y., Yarranton, H.W., “Regular solution model for asphaltene precipitation from bitumens and solvents”, AIChE J. 49 (2003) 2948–2956.

Alboudwarej, H., “Asphaltene deposition in flowing system”, Ph.D. Thesis, University of Calgary, Calgary, Canada, April 2003.

Andersen, S.I., Birdi, K.S., “Aggregation of Asphaltenes as Determined by Calorimetry”, Journal of Colloid Interface Science, 1991, 142(2), 497.

Andersen, S. I., “Hysteresis in Precipitation and Dissolution of Petroleum Asphaltenes”, Fuel Sci. Technol. Intl., 1992, 10, 1743−1749.

Andersen, S. I.; Stenby, E. H. Hysteresis in Asphaltene Precipitation and Redissolution. Proceedings of the Canadian Chemical Engineering Conference, October 1994, Calgary.

Andersen, S.I. and Speight, J.G., Thermodynamic Models For Asphaltene Solubility And Precipitation, Journal of Petroleum Science And Engineering, 22, 1999, 53–66

Badre, S, Goncalves, C.C., Norinaga, K., Gustavson, G., Mullins, O.C., “Molecular size and weight of asphaltene and asphaltene solubility fractions from coals, crude oils and bitumen”. Fuel 2006, 85(1), 1-11.

Barton, A.F.M., “CRC Handbook of Solubility parameters and other cohesion parameters”, Second Edition, CRC Press, 1991, p84-85.

Beck, J., Svrcek, W.Y., Yarranton, H.W., "Hysteresis in Asphaltene Precipitation and Redissolution," Energy & Fuels, 19(3), 2005, 944-947.

Browarzik, D., Laux, H., Rahimian, I.: "Asphaltene flocculation in crude oil systems," Fluid Phase Equilibria (1999) 154, 285-300.

Browarzik, C., Browarzik, D., "Modeling the Onset of Asphaltene Flocculation at High Pressure by an Association Model, Petroleum Science and Technology, 2005, 23, 795–810.

Buckley, J.S.: "Microscopic Investigation of the Onset of Asphaltene Precipitation," Fuel Sci. & Tech. Internat., 1996, 14, 55-74.

Buckley, J.S., Wang, J.X., and Creek, J.L., "Solubility of the Least Soluble Asphaltenes," Chapter 16 in Asphaltenes, Heavy Oils and Petroleomics; Mullins, O. C.; Sheu, E. Y.; Hammami, A.; Marshall, A. G., Eds.; Springer: New York, 2007

Chastko, P. A., "Developing Alberta's Oil Sands: From Karl Clark to Kyoto", University of Calgary Press, 2005.

Cimino, R., Correra, S., Sacomani, P.A., "Thermodynamic modeling for prediction of asphaltene deposition in live-oils", Proceedings of the SPE International Symposium on Oilfield Chemistry, San Antonio, TX, USA, 14–17 February 1995, 499–512.

Dean, J.A., "Lange's Handbook of Chemistry", McGraw-Hill, 15th Edition, 1999

Developer's Guide To VMG Extension Property, Virtual Materials Group, Calgary, Canada.

Flory, P. J., ''Thermodynamics of High Polymer Solutions,'' J. of Chem. Physics, 1941, 9, 660.

Gray, M.R., "Upgrading Petroleum Residues and Heavy Oils", Marcel Dekker, New York, 1994.

Gupta, A.K., "A model for asphaltene Flocculation Using an Equation of State", M.Sc. Thesis, Department of Chemical and Petroleum Engineering, University of Calgary, 1986.

Hammami, A., Ratulowski, J., "Precipitation and deposition of asphaltene in production systems: A flow assurance overview." Chapter 23 in Asphaltenes, Heavy Oils and Petroleomics; Mullins, O. C.; Sheu, E. Y.; Hammami, A.; Marshall, A. G., Eds.; Springer: New York, 2007.

Hildebrand, H.J., "Solubility. XII. Regular Solutions", J. Amer. Chem. Soc., 1929, 51-66.

Hirschberg, A., Dejong, L.N.J., Schipper, B.A., Meijer, J.G., Influence of Temperature and Pressure on Asphaltene Flocculation, SPE J., 1984, 24, 283-293.

Huggins, M. L., ‘‘Solutions of Long Chain Compounds’’, J. of Chem. Physics, 1941, 9, 440.

Ignasiak, T., Ruo, T.C.S., Strausz, O.P., “Investigation of Alberta Oil Sand Asphaltenes Using Thermal Degradation Reactions”, American Chemical Society, 1979, 24, 178

Janardhan, A.S. and Mansoori, G.A.: "Fractal Nature of Asphaltene Aggregation," Journal of Petroleum Science and Engineering, 1993, 9, 17-27

Kawanaka, S., Park, S.J., and Mansoori, G.A.: "Organic Deposition from Reservoir Fluids: A Thermodynamic Predictive Technique," SPE (1991) 5, 185-194.

Leontaritis, K.J. and Mansoori, G.A.: "Asphaltene Flocculation During Oil Production and Processing: A Thermodynamic - Colloidal Model," paper SPE 16258 presented at the 1987 SPE Internat. Symp. on Oilfield Chem., San Antonio, 4-6 Feb.

Leontaritis, K.J. and Mansoori, G.A.: "Asphaltene Deposition: A Survey of Field Experiences and Research Approaches," J. Pet. Sci. Eng., 1988, 1, 229-239.

Leontaritis, K.J. and Mansoori, G.A.: "Fast Crude-Oil Heavy-Component Characterization Using Combination of ASTM, HPLC, and GPC Methods," J. Pet. Sci. Eng., 1989, 2, 1-12.

Mannistu, K.D., Yarranton, H.W., and Masliyah, J.H., "Solubility Modeling of Asphaltenes in Organic Solvents", Energy and Fuels (1997) 11, 615-622.

Mansoori, G.A.: "Modeling of asphaltene and other heavy organic depositions," J. Pet. Sci. Eng., 1997, 17, 101-111.

Mitchell, D.L. and Speight, J.G., "The solubility of asphaltenes in hydrocarbon solvents," Fuel (1973) 52, 149-152.

Mullins, O.C., et al., "Asphaltenes, Heavy Oils and Petroleomics", Springer, 2007.

Nellensteyn, F.J., "The constitution of asphalt", Journal of the Institute of Petroleum Technology 10, 1924, p. 311.

Nghiem, L.X.; Hassam, M.S.; Nutakki, R., "Efficient Modeling of Asphaltene Precipitation", SPE#26642, 68th Anuual Technical Conference and Exhibition of SPE, Houston, Texas, October 3-6, 1993.

NIST Chemistry webbook - http://webbook.nist.gov/chemistry/

Nji, G. N.; Svrcek, W. Y.; Yarranton, H. W.; Satyro, M. A., "Characterization of Heavy Oils and Bitumens. 1. Vapor Pressure and Critical Constant Prediction Method for Heavy Hydrocarbons", Energy and Fuels 2008, 22 (5) 3559

Pedersen, K. S., Christensen, P.L., “Phase behaviour of petroleum reservoir fluids” CRC Press, 2007.

Peng, D.Y., Robinson, D.B.A., “New two-constant equation of state”, Ind. Eng. Chem. Fundam., 1976, 15, 59–64.

Peramanu, S., Singh, C., Agrawala, M. and Yarranton, H.W., “Investigation on the Reversibility of Asphaltene Precipitation” Energy and Fuels, 2001, 15 (4), 910–917.

Pfeiffer, J.P., Saal, R.N.J., “Asphaltic Bitumens as Colloid System”, Journal of Physical Chemistry, 1940, 44, 140.

Pinkston, K.S., Duan, P., Gallardo, V. A., Habicht,S. C., Tan, X., Qian, K., Gray, M., M llen, K., Kenttmaa, H. I., “Analysis of Asphaltenes and Asphaltene Model Compounds by Laser-Induced Acoustic Desorption/Fourier Transform Ion Cyclotron Resonance Mass Spectrometry”, Energy and Fuels (2009), Publication Date (Web): September 16, 2009

Qin, X., P. Wang, K. Sepehrnoori, G.A. Pope, “Modeling Asphaltene Precipitation in Reservoir Simulation” Ind. Eng. Chem. Res., 2000, 39 (8), 2644–2654.

Rachford, H.H., Rice, J.D., “Procedure for use of electronic digital computers in calculating flash vaporization hydrocarbon equilibrium”, J. Pet. Technol., October 1952. Technical Note 136.

Rastegari, K., “Measurement and modeling of asphaltene flocculation from Athabasca bitumen”, M.Sc. thesis, Department of Chemical and Petroleum Engineering, University of Calgary, 2003.

Rastegari, K., Svrcek. W.Y., Yarranton, H.W., "Kinetics of Asphaltene Flocculation," Ind. Eng. Chem. Res., 43, 2004, 6861-6870.

Romanova, U.G., Valinasab, M., Stasiuk, E.N., Yarranton, H.W., Schramm, L.L., Shelfantook, W.E., "The Effect of Bitumen Extraction Shear Conditions on Froth Treatment Performance," Paper No. 2004-028, 55th Canadian International Petroleum Conference, Calgary, AB, June 8-10, 2004.

Sabbagh, O., “An Eos Approach For Modeling Asphaltene Precipitation”, M.Sc. thesis, Department of Chemical and Petroleum Engineering, University of Calgary, 2004.

Sabbagh, O., Akbarzadeh, K., Badamchi-Zadeh, A., Svrcek, W. Y., Yarranton, H. W., “Applying the PR-EoS to Asphaltene Precipitation from n-Alkane Diluted Heavy Oils and Bitumens”, Energy and Fuels, 2006, 20 (2), 625-634.

Scatchard, G., “Equilibria in Non-electrolyte Solutions in Relation to the Vapor Pressures and Densities of the Components.”, Chem. Rev., 1931, 28, 321.

Sirota, E.B., “Physical Structure of Asphaltenes” Energy and Fuels, 2005, 19 (4), 1290–1296.

Smith, J. M., and van Ness, H. C., “Introduction to Chemical Engineering Thermodynamics”, McGraw-Hill, New York (1987)

Speight, J.G., “The Desulfurization of Heavy Oils and Residua”, CRC Press, 1999.

Strausz, O.P., Mojelsky, T.W., and Lown, E.M., “The Molecular Structure of Asphaltene: an Unfolding Story”; Fuel, 1992, Vol. 71, 1362.

Szewczyk, V.; Behar, E., Compositional Model for Predicting Asphaltenes Flocculation, Fluid Phase Equilibria, 1999, 158-160, 459-469.

Vasily Simanzhenkov and Raphael Idem., “Crude Oil Chemistry”, Marcel-Dekker, 2003, p. 328

Verdier, S., Duong, D., Andersen, S.I., “Experimental Determination of Solubility Parameters of Oils as a Function of Pressure”, Energy and Fuels, 2005, 19, 1225-1229.

VMGSim Process Simulator, Version 5.0, 2009

VMGThermo Programmers Manual, Virtual Material Group, Calgary, Canada.

Whitson, C.H., "Characterizing Hydrocarbon Plus Fractions", SPE# 12233, SPE Journal, August 1983, 683-694.

Wiehe, I.A., 1992 Ind. Eng. Chem. Res., 1992, 31, 530-536.

Wiehe, I.A., Liang, K.S., Asphaltenes, Resins, and Other Petroleum macromolecules, Fluid Phase Equilibria, 1996, 117, 201-210.

Wong, D.S., and Sandler, S.I.A., "Theoretically correct new mixing rule for cubic equations of state for both highly and slightly non-ideal mixtures", AIChE J. 38 (1992), 671–680.

Wu, J., Prausnitz, J.M., and Firoozabadi, A.: "Molecular Thermodynamics of Asphaltene Precipitation in Reservoir Fluids. AIChE J, 2000, 46, 197-209.

Wu, J.; Prausnitz, J. M.; Firoozabadi, A. "Molecular-Thermodynamic Framework for Asphaltene-Oil Equilibria" AIChE J. 1998, 44, 1188-1199.

Yarranton, H. W., H. Alboudwarej and R. Jakher, "Investigation of Asphaltene Association with Vapour Pressure Osmometry and Interfacial Tension Measurements," Ind. Eng. Chem. Res., 2000, 39, 2916-2924.

Yarranton, H.W., Fox, W.A., Svrcek, W.Y., “Effect of Resins on Asphaltene Self-Association and Solubility”, Can. J. Chem. Eng., 2007, 85(5), 635-642.

Yarranton, H.W.; Masliyah, J.H., “Molar Mass Distribution and Solubility Modeling of Asphaltenes”, AIChE J. 1996, 42, 3533-3543.

Zou, X-Y., Shaw, J. M., “Dispersed Phases and Dispersed Phase Deposition Issues Arising in Asphaltene Rich Hydrocarbon Fluids”, Petroleum Science and Technology, 2004, 22:7, 759-771.

APPENDIX: Error Analysis

The confidence intervals for the solvent contents of asphaltene-rich phases are presented in Section A and B for the asphaltene-solvent and diluted bitumen systems, respectively. The accuracy of the model results in comparison with the measured were assessed in terms of the average absolute deviation (AAD) and are presented in Section C.

A. Error Analysis of Composition Experiments for n-Alkane/Toluene/Asphaltene Systems

Table A-1 presents the means and standard deviation of the measured solvent contents in the asphaltene-rich phase of n-alkane/toluene/asphaltene. The mean for each pair of measurements is calculated using:

$$\bar{x} = \frac{1}{n}\sum_{i=1}^{n} x_i \qquad \textbf{(1)}$$

where n is the number of repeat measurements for each experiment set and x_i is a measured value. The sample variance for each pair of measurements is given by:

$$s^2 = \frac{1}{n-1}\sum_{i=1}^{n} (x_i - \bar{x})^2 \qquad \textbf{(2)}$$

The standard deviation is the square root of the sample variance.

Table A-1: Mean and standard deviation for the measured solvent content in the asphaltene-rich phase of n-alkane / toluene/ asphaltene systems.

Solvent (Init. N-alk vol fr)	Asphaltene type	Data-1	Data-2	Mean	Std. Dev
Heptane (0.5)	C7	5.8	5.9	5.85	0.07
Heptane (0.65)	C7	6.9	6.5	6.7	0.28
Heptane (0.8)	C7	7.2	6.2	6.7	0.71
Pentane (0.8)	C7	5.3	6.5	5.9	0.85
Decane (0.8)	C7	5.1	7.1	6.1	1.41
Heptane (0.8)	C5	5.4	5.8	5.6	0.28

However, if we assume that the population of error is the same for all of the measurements (not just for each pair) then the sample variance is smaller and can be determined as follows:

$$s = \sqrt{\frac{1}{m-1}\sum_{i=1}^{n}(x_{ji} - \bar{x}_j)^2} \qquad \textbf{(3)}$$

where $\bar{x}_j$ is the mean of each repeat measurement set and m is the total number of measurements.

The confidence intervals for each mean value based on a pair of measurements is calculated based on the sample variance and the *t-distribution* as given below:

$$\bar{x} - t_{(\alpha/2,\nu)}\frac{s}{\sqrt{n}} \le \mu \le \bar{x} + t_{(\alpha/2,\nu)}\frac{s}{\sqrt{n}} \qquad \textbf{(4)}$$

where μ is the correct mean, $\nu = n - 1$ and $\alpha = 1 - (\%\text{conf}/100)$; for example, for 95% confidence, $\alpha = 0.05$.

For the data presented in **Table A-1** and 95% confidence, α/2 = 0.025, v = 11 and t is calculated as 2.2 from t-distribution table (Dean, J.A., 1999). For each measurement, the distribution was sampled twice and n= 2. The confidence interval is then ±0.9 and the weight percent of solvent in the asphaltene-rich phase of n-alkane/toluene/asphaltene is 6.1 ± 0.9 %.

B. Error Analysis of Composition Experiments for Diluted Bitumen Systems

The statistical analysis of the measured solvent contents in the asphaltene-rich phase of diluted bitumen systems is presented in **Table A-2**. All the calculations were done as was explained in Section A.

Table A-2: Mean and standard deviation of the data for composition of solvent in the asphaltene-rich phase of diluted bitumen system.

Heptane dilution (g/g)	Data-1	Data-2	Mean	Std. Dev
1.9	12.1	5.6	8.9	4.60
4.0	10.3	14.7	12.5	3.11
40.0	15.5	10.8	13.2	3.32
40.0 (no additional solvent)	9.1	9.3	9.2	0.14

For 95% confidence, α/2 = 0.025, v = 7 and t is calculated as 2.36 from t-distribution table (Dean, J.A., 1999). A pair of repeats are considered for each measurement set, so n=2. The confidence interval is calculated as ±4.1. The weight percent of solvent in the asphaltene-rich phase of diluted bitumen is 11 ± 4 %.

C. Average Absolute Deviation of Model Results

The average absolute deviation was calculated for the model results presented in Chapter 6 using the following equation:

$$AAD = \frac{1}{n}\sum_{i=1}^{n}\left|FP_{calculated} - FP_{measured}\right|_i \quad \textbf{(5)}$$

where $FP_{calculated}$ is the value of fractional precipitation calculated from the model, $FP_{measured}$ is the measured value of fractional precipitation and n is the number of data points.

Table A-3 and **Table A-4** tabulate the average absolute deviation values between the experimental results and model results of fractional asphaltene precipitation from asphaltene/n-alkane/toluene system. The model was fitted to the Athabasca Asphaltenes (mwavg = 5900)/Toluene/n-heptane data at 0 °C, 23 °C and 50 °C with an AAD of 0.0315, 0.0422 and 0.0254 respectively. The AAD values are higher for solvents n-octane and n-decane, where the model predictions are the least accurate. The average AAD is 0.0788. The AAD values of the old model are also shown for comparison.

Table A-3: Average absolute deviation of model results for asphaltene/n-alkane/toluene system.

System	AAD	
	New model	Old model
Athabasca Asphaltenes (mwavg = 5900)/Toluene/n-pentane, 23 °C, 1 atm, 10 g/lit Asphaltenes	0.0612	0.0180
Athabasca Asphaltenes (mwavg = 5900)/Toluene/n-hexane, 23 °C, 1 atm, 10 g/lit Asphaltenes	0.0514	0.0505
Athabasca Asphaltenes (mwavg = 5900)/Toluene/n-heptane, 23 °C, 1 atm, 10 g/lit Asphaltenes	0.0412	0.0745
Athabasca Asphaltenes (mwavg = 5900)/Toluene/n-octane, 23 °C, 1 atm, 10 g/lit Asphaltenes	0.1544	0.0386
Athabasca Asphaltenes (mwavg = 5900)/Toluene/n-decane, 23 °C, 1 atm, 10 g/lit Asphaltenes	0.1678	0.0616
Athabasca Asphaltenes (mwavg = 7900)/Toluene/n-heptane, 0 °C, 1 atm, 10 g/lit Asphaltenes	0.0315	0.0238
Athabasca Asphaltenes (mwavg = 7900)/Toluene/n-heptane, 23 °C, 1 atm, 10 g/lit Asphaltenes	0.0422	0.0218
Athabasca Asphaltenes (mwavg = 7900)/Toluene/n-heptane, 50 °C, 1 atm, 10 g/lit Asphaltenes	0.0254	0.0137
Athabasca, UW-Asphaltenes (mwavg = 7900)/Toluene/n-heptane, 23 °C, 1 atm, 10 g/lit Asphaltenes	0.1123	0.0166
Athabasca, Son.W-Asphaltenes (mwavg = 7600)/Toluene/n-heptane, 23 °C, 1 atm, 10 g/lit Asphaltenes	0.1048	0.1102
Athabasca, Sox.W-Asphaltenes (mwavg = 9100)/Toluene/n-heptane, 23 °C, 1 atm, 10 g/lit Asphaltenes	0.0568	0.0979
Venezuela1 Asphaltenes (mwavg =10000)/Toluene/n-heptane, 23 °C, 1 atm, 10 g/lit Asphaltenes	0.0413	0.0486
Venezuela2 Asphaltenes (mwavg =7700)/Toluene/n-heptane, 23 °C, 1 atm, 10 g/lit Asphaltenes	0.0466	0.0525
Russia Asphaltenes (mwavg =7100)/Toluene/n-heptane, 23 °C, 1 atm, 10 g/lit Asphaltenes	0.0638	0.0353
Cold Lake Asphaltenes (mwavg =7900)/Toluene/n-heptane, 23 °C, 1 atm, 10 g/lit Asphaltenes	0.0680	0.0681
Indonesia Asphaltenes (mwavg =4600)/Toluene/n-heptane, 23 °C, 1 atm, 10 g/lit Asphaltenes	0.2384	0.0344

UW – Unwashed; Son.W - Sonicator washed; Sox.W - Soxhlet washed

mwavg - Average molar mass of asphaltene at 50 °C

Table A-4: Average absolute deviation of model results for Athabasca asphaltene/n-heptane/toluene system at different asphaltene concentrations.

System	AAD	
	New model	Old model
Athabasca Asphaltenes (mwavg = 5900)/Toluene/n-heptane, 23 °C, 1 atm, 0.20 Toluene Volume fraction	0.0469	0.1249
Athabasca Asphaltenes (mwavg = 5900)/Toluene/n-heptane, 23 °C, 1 atm, 0.25 Toluene Volume fraction	0.0735	0.1304
Athabasca Asphaltenes (mwavg = 5900)/Toluene/n-heptane, 23 °C, 1 atm, 0.33 Toluene Volume fraction	0.0851	0.0803
Athabasca Asphaltenes (mwavg = 5900)/Toluene/n-heptane, 23 °C, 1 atm, 0.40 Toluene Volume fraction	0.0625	0.0101